

1 **The Open-source Data Inventory for Anthropogenic Carbon dioxide (CO<sub>2</sub>), version**  
2 **2016 (ODIAC2016): A global, monthly fossil-fuel CO<sub>2</sub> gridded emission data product for**  
3 **tracer transport simulations and surface flux inversions**

4  
5 Tomohiro Oda<sup>1,2</sup>, Shamil Maksyutov<sup>3</sup> and Robert J. Andres<sup>4</sup>

6  
7 1: Global Modeling and Assimilation Office, NASA Goddard Space Flight Center, Greenbelt,  
8 MD, USA.

9 2: Goddard Earth Sciences Technology and Research, Universities Space Research  
10 Association, Columbia, MD, USA

11 3: Center for Global Environmental Research, National Institute for Environmental Studies,  
12 Tsukuba, Ibaraki, Japan

13 4: Carbon Dioxide Information Analysis Center, Oak Ridge National Laboratory, Oak Ridge,  
14 TN, USA

15  
16 Corresponding author: T. Oda ([tomohiro.oda@nasa.gov](mailto:tomohiro.oda@nasa.gov))

17  
18 **Abstract**

19 [The](#) Open-source Data Inventory for Anthropogenic CO<sub>2</sub> (ODIAC) is a global high-spatial  
20 resolution gridded emission data product that distributes carbon dioxide (CO<sub>2</sub>) emissions  
21 from fossil fuel combustion. The emission spatial distributions are estimated at a 1×1 km  
22 spatial resolution over land using power plant profiles (emission intensity and geographical  
23 location) and satellite-observed nighttime lights. This paper describes the [year 2016](#) version  
24 of the ODIAC emission data product (ODIAC2016) and presents analyses that help guiding  
25 data users, especially for atmospheric CO<sub>2</sub> tracer transport simulations and flux inversion  
26 analysis. Since the original publication in 2011, we have made modifications to our emission  
27 modeling framework in order to deliver a comprehensive global gridded emission data  
28 product. Major changes from the 2011 publication are 1) the use of emissions estimates made  
29 by the Carbon Dioxide Information Analysis Center (CDIAC) at [the](#) Oak Ridge National  
30 Laboratory (ORNL) by fuel type (solid, liquid, gas, cement manufacturing, gas flaring and  
31 international aviation and marine bunkers), 2) the use of multiple spatial emission proxies by  
32 fuel type such as nightlight data specific to gas flaring and ship/aircraft fleet tracks and 3) the  
33 inclusion of emission temporal variations. Using global fuel consumption data, we  
34 extrapolated the CDIAC emissions [estimates](#) for the recent years and produced the  
35 ODIAC2016 emission data product that covers 2000-2015. Our emission data can be viewed  
36 as an extended version of CDIAC gridded emission data product, which should allow data  
37 users to impose global fossil fuel emissions in more comprehensive manner than original  
38 CDIAC product. Our new emission modeling framework allows us to produce future versions  
39 of ODIAC emission data product with a timely update. Such capability has become more  
40 significant given the CDIAC/[ORNL](#)'s shutdown. ODIAC data product could play an  
41 important role to support carbon cycle science, especially modeling studies with space-based  
42 CO<sub>2</sub> data collected near real time by ongoing carbon observing missions such as Japanese  
43 Greenhouse Observing SATellite (GOSAT), NASA's Orbiting Carbon Observatory 2 (OCO-  
44 2) and upcoming future missions. The ODIAC emission data product [including the latest](#)  
45 [version of the ODIAC emission data \(ODIAC2017, 2000-2016\)](#), is distributed from  
46 <http://db.cger.nies.go.jp/dataset/ODIAC/> with a DOI.

Deleted: latest

1  
2 **1. Introduction**  
3

4 Carbon dioxide (CO<sub>2</sub>) emissions from fossil fuel combustion are the main cause for the  
5 observed increase in atmospheric CO<sub>2</sub> concentration. The Carbon Dioxide Information  
6 Analysis Center (CDIAC) at [the](#) Oak Ridge National Laboratory (ORNL) estimated that the  
7 global total fossil fuel CO<sub>2</sub> emissions (FFCO<sub>2</sub>; fuel combustion, cement production and gas  
8 flaring) in the year 2014 was 9.855 PgC based on fuel statistics data published by United  
9 Nation (U.N.) (Boden et al., 2017). This FFCO<sub>2</sub> estimate often serves as a reference in carbon  
10 budget analysis, especially for inferring CO<sub>2</sub> uptake by terrestrial biosphere and oceans (e.g.  
11 Ballantyne et al., 2012; Le Quéré et al., 2016). The Global Carbon Project for example  
12 estimated that approximately 55% of the carbon released to the atmosphere (FFCO<sub>2</sub> plus  
13 emissions from land use change) was taken up by natural sinks over the past decade (2006-  
14 2015) (Le Quéré et al., 2016).

15 Similarly, FFCO<sub>2</sub> estimates serve as a reference in atmospheric CO<sub>2</sub> flux inversion analysis  
16 where the location and size of natural sources and sinks are estimated using atmospheric CO<sub>2</sub>  
17 data and atmospheric transport models (e.g. Tans et al., 1990; Bousquet et al., 1999; Gurney  
18 et al., 2002; Baker et al., 2006). In the conventional inversion method, unlike land and  
19 oceanic fluxes, FFCO<sub>2</sub> is a given quantity and never optimized (e.g. Gurney et al., 2005).  
20 FFCO<sub>2</sub> thus needs to be accurately quantified and given in space and time to yield robust  
21 estimates of natural fluxes (Gurney et al., 2005). Accurately prescribing FFCO<sub>2</sub> has become  
22 more critical because of the use of spatially and temporally dense CO<sub>2</sub> data from a wide  
23 variety of observational platforms (ground-based, aircrafts and satellites), which inform not  
24 only background levels of CO<sub>2</sub> concentration, but also CO<sub>2</sub> contributions from anthropogenic  
25 sources (e.g. Schneising et al., 2013; Janardan et al., 2016; Hakkarainen et al., 2016).  
26 Atmospheric transport models then need to be run at a higher spatiotemporal resolution than  
27 before to fully interpret and utilized CO<sub>2</sub> variability observed at synoptic to local scale to  
28 quantify sources and sinks (e.g. Feng et al. 2016; Lauvaux et al., 2016). FFCO<sub>2</sub> data thus  
29 needs to be accurately given at a high resolution so as not to cause biases in simulations.

30 Global FFCO<sub>2</sub> data are available in a gridded form from different institutions and research  
31 groups (e.g. CDIAC/ORNL and Europe's Joint Research Center (JRC)) and those gridded  
32 emission data are often based on disaggregation of national (or sectoral) emissions (e.g.  
33 Andres et al., 1996; Rayner et al., 2010; Oda and Maksyutov 2011; Janssens-Maenhout et al.,  
34 2012; Kurokawa et al., 2013; Asefi-Najafabady et al., 2014). The emission spatial  
35 distributions are often estimated using spatial proxy data that approximate the location and  
36 intensity of human activities (hence, CO<sub>2</sub> emissions) (e.g. population, nighttime lights and  
37 gross domestic production (GDP)) and/or geolocation of specific emission sources (e.g.  
38 power plant, transportation, cement production/industrial facilities and gas flares). CDIAC  
39 gridded emission data product for example is based on an emission disaggregation using  
40 population density at a 1×1 degree resolution (Andres et al., 1996). The Emission Database  
41 for Global Atmospheric Research (EDGAR, <http://edgar.jrc.ec.europa.eu/>) estimates  
42 emissions on the emission sectors specified by the Intergovernmental Panel on Climate  
43 Change (IPCC) methodology instead of fuel type and use spatial proxy data and geospatial  
44 data such as point and line source location at a 0.1×0.1 degree (Janssens-Maenhout et al.,  
45 2012).

46 Satellite-observed nighttime light data has been identified as an excellent spatial indicator  
47 for human settlements and intensities of some specific human activities (e.g. Elvidge et al.,  
48 1999, 2009) and has been used to infer the associated CO<sub>2</sub> emissions or their spatial

Deleted:

Deleted: s

1 distributions (e.g. Doll et al., 2000, Ghosh et al., 2010, Rayner et al., 2010). Oda and  
2 Maksyutov (2011) proposed a combined use of power plant profiles (power plant emission  
3 intensity and geographical location) and nighttime light data to achieve a global high-spatial  
4 resolution emission field. The decoupling of the point source emission which often have less  
5 spatial correlation with population (hence, nighttime light), yields improved high-resolution  
6 emission fields that show an improved agreement with the U.S. 10km Vulcan emission  
7 product developed by Gurney et al. (2009) (Oda and Maksyutov 2011). Based on Oda and  
8 Maksyutov (2011), we initiated [the high-resolution emission data development](#) (named as the  
9 Open-source Data Inventory for Anthropogenic CO<sub>2</sub>, ODIAC) under the Japanese  
10 Greenhouse Gases Observing SATellite (GOSAT, Yokota et al., 2009) at the Japanese  
11 National Institute for Environmental Studies (NIES). The original purpose of the emission  
12 data development was to provide an accurate prior FFCO<sub>2</sub> field for global and regional CO<sub>2</sub>  
13 inversions using the column-averaged CO<sub>2</sub> (X<sub>CO<sub>2</sub></sub>) data collected by GOSAT. Since 2009, the  
14 ODIAC emission data product has been used for the inversion for the official GOSAT Level  
15 4 (surface CO<sub>2</sub> flux) data production (Takagi et al., 2009; Maksyutov et al., 2013), NOAA's  
16 CarbonTracker (Peters et al., 2007) as a supplementary FFCO<sub>2</sub> data, as well as dozens of  
17 published works (e.g. Saeki et al., 2013; Thompson et al., 2015; Feng et al., 2016; Feng et al.,  
18 2017; Shirai et al., 2017) including several urban scale modeling studies (e.g. Ganshin et al.  
19 2010; Oda et al., 2012; Brioude et al., 2013; Lauvaux et al., 2016; Janardanan et al., 2016;  
20 Oda et al., 2017).

21 In response to increasing needs from the CO<sub>2</sub> modeling research community, we have  
22 upgraded and modified our modeling framework in order to produce a global, comprehensive  
23 emission data product on timely manner, while our flagship high-resolution emission  
24 modeling approach remains as the same. In this manuscript, we describe the [year 2016](#),  
25 [version of the ODIAC emission data product \(ODIAC2016, 2000-2015\), which was the latest](#)  
26 [version of the ODIAC emission data at the time of the submission of this manuscript](#), along  
27 with the emission modeling framework we are currently based on, highlighting  
28 changes/differences from Oda and Maksyutov (2011). [Currently the updated, year 2017](#)  
29 [version of the ODIAC emission data \(ODIAC2017, 2000-2016\) are available. This](#)  
30 [manuscript however provides the sufficient details of how we developed ODIAC2017 with](#)  
31 [updated information](#).

## 32 33 34 **2. Emission modeling framework**

35  
36 Fig. 1 illustrates our current ODIAC emission modeling framework (we defined it as  
37 "ODIAC 3.0 model", in contrast to the original version). Major changes/differences from Oda  
38 and Maksyutov (2011, ODIAC v1.7) are 1) the use of emissions estimates made by the  
39 CDIAC/[ORNL](#) (rather than our own emission estimates), 2) the use of multiple spatial  
40 emission proxies in order to distribute CDIAC [national](#) emissions [estimates](#) made by fuel type,  
41 and 3) the inclusion of emission temporal variations (version 1.7 only indicates annual  
42 emission fields). Given CDIAC [emission](#) estimates have been one of well-respected, widely-  
43 used in the carbon research community (e.g. Ballantyne et al., 2012; Le Quéré et al., 2016),  
44 our philosophy in our emission data development is we develop and deliver an extended,  
45 comprehensive global gridded emission data product, fully utilizing CDIAC emissions data  
46 (e.g. emission estimates in both tabular and gridded forms). We also extend CDIAC emission  
47 data where possible. Our emission modeling framework was also designed to produce an  
48 [annually-updated](#) emission data product in a timely manner, [Given the discontinuity of future](#),

Deleted: an

Deleted: s

Deleted: a

Deleted: latest

Deleted: /upgrade

Deleted: , with updated information

1 updated CDIAc emission data, we believe our emission data production capability of  
 2 producing an extended product of the CDIAc emission data is significant.  
 3 Starting with national emission estimates as an input, our model framework achieves  
 4 monthly, global FFCO<sub>2</sub> gridded fields via preprocessing, and spatial and temporal  
 5 disaggregation. CDIAc national estimates made by fuel type (liquid, gas, solid, cement  
 6 production, gas flare and international bunker emissions) are further divided into an extended  
 7 set of ODIAC emission categories (point source, non-point source, cement production, gas  
 8 flare, international aviation and marine bunker (further described in Section 3). It is important  
 9 to note that ODIAC2016 carries emissions from international bunker (international marine  
 10 bunker and aviation, often accounts for a few percent of the global total emissions), which are  
 11 not included in the CDIAc gridded emission data products (CDIAc gridded emission data  
 12 only indicate national emissions and international bunker emissions are often not considered  
 13 to be a part of national emissions in an international convention). With the inclusion of  
 14 international bunker emissions, we provide a more comprehensive global gridded emission  
 15 field. We extended the CDIAc national estimates over the recent years that was not yet  
 16 covered in the version of CDIAc gridded data (2014-2016), in order to support near-real time  
 17 CO<sub>2</sub> simulations/analysis. Emissions are then spatially distributed using a wide variety of  
 18 spatial data (e.g. point source geographical location, nighttime light data and flight/ship tracks,  
 19 further described in Section 4). We adopt an emission seasonality from existing emission  
 20 inventories for particular emission categories (further described in Section 5).  
 21 In the following sections (Section 3-5), we describe how ODIAC2016 was developed. It is  
 22 important to note that ODIAC2016 is based on the best available data at the time of the  
 23 development (ODIAC2016 was released in September 2016). Thus, some of the emission  
 24 estimates and underlying data used in ODIAC2016 might have been outdated. For traceability  
 25 purpose, data used in this development, their versions/editions, and data sources are  
 26 summarized in Appendix A. Following the results and evaluation section (Section 6), we  
 27 discuss caveats and current limitations in our modeling framework/emission data product  
 28 (Section 7), and then describe how we will update the ODIAC emission data product with  
 29 updated fuel statistics and/or emission information (Section 8). Atmospheric CO<sub>2</sub> inversion  
 30 studies recently published (e.g. Maksyutov et al., 2013) and operational assimilation systems  
 31 such as NOAA's CarbonTracker (<https://www.esrl.noaa.gov/gmd/ccgg/carbontracker/>) often  
 32 focus on time periods after 2000. We thus put a priority to produce emission data after year  
 33 2000 with regular update upon the availability of updated emission and fuel statistical data  
 34 and deliver the emission product to the science community, instead of developing a longer  
 35 term emission data product. Future versions of ODIAC data however might have a longer,  
 36 extended time coverage. Currently the ODIAC data are provided in two data formats: 1)  
 37 global 1×1 km (30 arc second) monthly data in the GeoTIFF format (only includes emissions  
 38 over land) and 2) 1×1 degree annual (12 month) data in the NetCDF format (includes  
 39 international bunker emissions). The 1×1 degree annual data are aggregated from the 1×1 km  
 40 product. The improvements with the use of improved nighttime light data in the 1×1 km data  
 41 were documented in Oda et al. (2012). This manuscript thus focuses on the comprehensive  
 42 global FFCO<sub>2</sub> fields at a 1×1 degree, otherwise specified.

- Deleted: As
- Deleted: ODIAC
- Deleted: product
- Deleted: is based
- Deleted: , our emission data production capability
- Deleted: given the expected discontinuity of future CDIAc emission data.
- Deleted: s
- Deleted: estimates
- Deleted: s
- Deleted: Given recent most of
- Formatted: Not Highlight
- Deleted: a
- Formatted: Not Highlight
- Field Code Changed
- Formatted: Not Highlight
- Formatted: Not Highlight
- Formatted: Not Highlight
- Deleted: develop
- Formatted: Not Highlight
- Deleted: for years
- Formatted: Not Highlight
- Deleted: ed
- Formatted: Not Highlight
- Deleted: years
- Formatted: Not Highlight
- Deleted: ,
- Formatted: Not Highlight
- Deleted: w
- Formatted: Not Highlight
- Deleted:
- Formatted: Not Highlight
- Deleted: in a timely manner
- Deleted: n

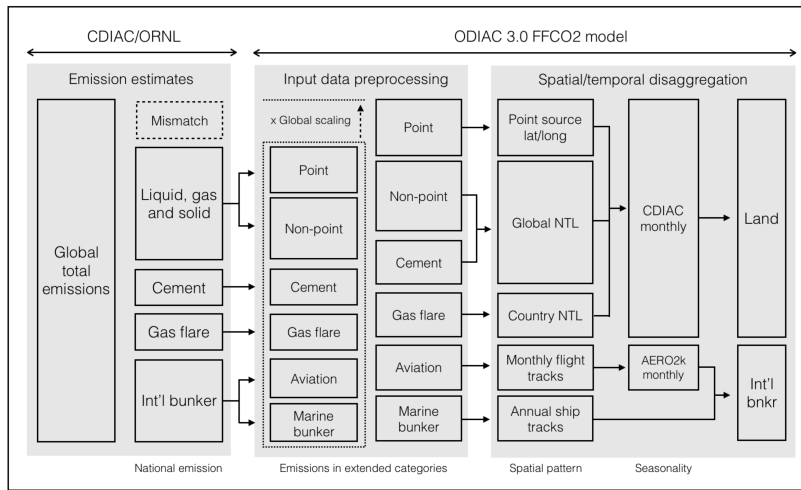


**Figure 1.** A schematic figure of the ODIAC emission modeling framework (defined as “ODIAC 3.0 FFCO2 model”). Starting with CDIAC national emission estimates made by fuel type (emission estimates), the CDIAC national emission estimates are first divided into extended ODIAC emission categories (input data processing, see Section 3). ODIAC 3.0 FFCO2 model then distributes the emissions in space and time, using point source geolocation information and spatial data depending on emission category such as nighttime light (NTL), and aircraft and ship fleet tracks (spatial disaggregation, see Section 4). The emission seasonality for emissions over land and international aviation were adopted from existing emission inventories (temporal disaggregation, see Section 5).

Deleted: A

Deleted: s

Deleted: s

Deleted: s

1  
2  
3  
4  
5  
6  
7  
8  
9  
10  
11  
12  
13  
14  
15  
16  
17  
18  
19  
20  
21

### 3. Emission estimates and input emission data preprocessing

#### 3.1 Emissions for 2000-2013

CDIAC FFCO2 emissions estimates are based on fuel statistic data published as United Nation Energy Statistics Database (Boden et al., 2017). Emission estimates are calculated on global, national and regional basis and by fuel type in the method described in Marland and Rotty (1984). CDIAC also provides their own gridded emission data products that indicate annual and monthly FFCO2 fields at a 1×1 degree (Andres et al., 1996; Andres et al., 2011). ODIAC2016 is primarily based on the year 2016 version of the CDIAC national estimates (Boden et al., 2016), which was the most up-to-date CDIAC emission estimates at the time of the data development (currently Boden et al. 2017 is the latest). We first aggregated the CDIAC national (and regional) emissions estimates to 65 countries and 6 geographical regions (North America, South and Central Americas, Europe and Eurasia, the Middle East, Africa, and Asia Pacific) defined in Oda and Maksyutov (2011) (see the country/region definitions are shown in Table 1 in Oda and Maksyutov 2011). In addition to the national and geographical categories, we decided to include Antarctic fishery emissions, which are from fishery activities over the Antarctic Ocean (< 60S, 1~ 4 kTC/yr over 1987-2007 by Boden et al., 2016), as an individual emission region and distributed in the same way as Andres et al.

1 (1996). Emissions from international bunker and aviation are not included in national  
2 emissions by international convention. Thus CDIAC gridded emission data products do not  
3 include the emissions from international bunker and aviation although [the CDIAC/ORNL](#)  
4 [does](#) have records of those emissions on national/regional basis. ODIAC2016 includes those  
5 emissions to achieve comprehensive global FFCO<sub>2</sub> gridded emission fields.

6 In CDIAC emission estimates, the global total emission and national total emissions are  
7 obtained by different calculation methods (global fuel production vs. apparent national fuel  
8 consumption, see Andres et al., 2012) and the CDIAC national totals do not sum to the  
9 CDIAC global total due to the difference in calculation method and inconsistencies in the  
10 underlying statistical data (e.g. import/export totals) (e.g. Andres et al., 2012). We thus  
11 calculate the difference between the global total and the sum of national totals and scaled up  
12 national totals to account for the difference. Andres et al. (2014) reported [global total](#)  
13 emission estimates calculated with production data (as opposed to apparent consumption  
14 data) have the smallest uncertainty (approximately 8% (2 sigma). It is thus used as the  
15 reference for global carbon budget analyses, (e.g. Le Quéré et al., 2016). Inversion analysis is  
16 an extended version of the global carbon budget analysis using atmospheric models. We thus  
17 believe that imposing transport models and/or inversion models in a consistent way with the  
18 global carbon budget analysis such as Le Quéré et al. (2016) has significance, although we  
19 sacrifice the accuracy of the national/regional emission estimates. Due to the global scaling,  
20 national totals in ODIAC2016 differ from the estimates originally reported by [the](#)  
21 [CDIAC/ORNL](#). The differences between the CDIAC global total and the sum of national  
22 emissions are often few percent and thus the magnitude of the scaling is often within the  
23 uncertainty range of national emissions (e.g. 4.0 to 20.2%, Andres et al., 2014). [The global](#)  
24 [scaling factor derived and used in this study are presented in Appendix A2.](#)

Deleted: is

### 25 26 3.2 Emissions for 2014-2015

27  
28 The year 2016 version of the CDIAC [emission](#) estimates only covers years to 2013 (Boden  
29 et al., 2016). We thus extrapolated the year 2013 CDIAC emissions to years 2014 and 2015  
30 using the year 2016 version of [the BP](#) global fuel statistical data (BP, 2017). Our emission  
31 extrapolation approach [is](#) the same as Myhre et al. (2009) and Le Quéré et al. (2016).

32 Emissions from cement production and gas flaring (approximately 5.7% and 0.6% of the  
33 2013 global total, Boden et al., 2016) were assumed to be as the same as year 2013.  
34 International bunker emissions were scaled using changes in national total emissions.

Deleted: are

### 35 36 3.3 CDIAC emission sector to ODIAC emission categories

37  
38 CDIAC national emission estimates (prepared by fuel type) were re-categorized to our own  
39 ODIAC emission categories (point source, nonpoint source, cement production, gas flare and  
40 international aviation and international marine bunker). Following Oda and Maksyutov  
41 (2011), the sum of emissions from liquid, gas and solid fuels was further divided into point  
42 source emissions and non-point source emissions. The total emissions from point sources  
43 were estimated using national total power plant emissions calculated using CARMA (Oda and  
44 Maksyutov, 2011). As mentioned earlier, CDIAC gridded emission data products only  
45 indicate national emissions and do not include international bunker emissions (Andres et al.,  
46 1996, Andres et al., 2011). In contrast, EDGAR provides bunker emissions in their gridded  
47 data product (JRC, 2017). Peylin et al. (2013) show some models include international bunker  
48 emissions and some do not, although the difference due to the inclusion/exclusion of the

1 international bunker emissions in the prescribed emissions could be corrected afterwards  
2 (Peylin et al., 2013). In ODIAC2016, we carry CDIAC international bunker emissions  
3 reported on country basis to achieve the complete picture of the global fossil fuel emissions.  
4 Country total bunker emissions (aviation plus marine bunker) were distributed using spatial  
5 proxy data adopted from other emission inventories described later (see [Section 4.3](#)).  
6 Although [the CDIAC/ORNL](#) does not report emissions from international aviation and  
7 marine bunker separately, we loosely estimated those two emissions using U.N. statistics. We  
8 estimated the fraction of aircraft emissions using jet fuel and aviation gasoline consumption  
9 and then the international bunker emissions were divided into aircraft and marine bunker  
10 emissions.

Deleted: s

#### 13 4. Spatial emission disaggregation

##### 15 4.1 Emissions from point sources, non-point sources and cement production

17 We define the sum of the emissions from solid, liquid and gas fuels as land emission (see  
18 Fig. 1). Land emissions are further divided into two emission categories (point source  
19 emissions and non-point source emissions) and then distributed [at a 1×1 km resolution](#) in the  
20 ways described in Oda and Maksyutov (2011): Point source emissions are mapped using  
21 power plant profiles (emission intensity and geographical location) [taken from the CARbon](#)  
22 [Monitoring and Action \(CARMA\) database \(Wheeler and Ummel, 2008\)](#) and non-point  
23 source emissions are distributed using nighttime light data collected by the Defense  
24 Meteorological Satellite Program (DMSP) satellites ([e.g. Elvidge et al., 1999](#)). To avoid a  
25 difficulty in emission disaggregation especially over bright regions in nighttime light data (e.g.  
26 cities), Oda and Maksyutov (2011) employed a product that does not have an instrument  
27 saturation issue, rather than regular nightlight product. ODIAC2016 employs the latest  
28 version of the special nighttime light product (Ziskin et al., 2010). The improved nighttime  
29 light data has mitigated the underestimation of emissions over dimmer areas seen in ODIAC  
30 v1.7 (Oda et al., 2010). Nighttime light data are currently available for multiple years (1996-  
31 97, 1999, 2000, 2002-03, 2004, 2005-06 and 2010). In ODIAC2016, due to the lack of  
32 information, [the](#) emissions from cement production were spatially distributed as a part of non-  
33 point source emissions, although those emissions should have been distributed as point  
34 sources. This needs to be fixed in future versions [of](#) ODIAC emission data.

Deleted: in

##### 36 4.2 Emissions from gas flaring

38 In the ODIAC v1.7, emissions from gas flaring were not considered (Oda and Maksyutov  
39 2011). Nighttime light pixels corresponding to gas flares often appear very bright and would  
40 result in creating strong point sources in emission data (Oda and Maksyutov, 2011). We thus  
41 identified and excluded those bright gas flare pixels before distributing land emissions, using  
42 another global nighttime light data product that was specifically developed for gas flares by  
43 National Oceanic and Atmosphere Administration (NOAA), National Centers for  
44 Environmental Information (NCEI, former National Geophysical Data Center (NGDC)) (Oda  
45 and Maksyutov, 2011). In ODIAC2016 we separately distributed CDIAC gas flare emissions  
46 using the [1×1 km nighttime-based gas flare maps developed for 65 individual countries](#)  
47 (Elvidge et al., 2009). Other than the 65 countries, [the](#) gas flare emissions were distributed as  
48 a part of land emissions.

Deleted:

Deleted:

1  
2 4.3 Emissions from international aviation and marine bunker  
3

4 Emissions from international aviation and marine bunker were distributed using aircraft and  
5 ship fleet tracks. International aviation emissions were distributed using the AERO2k  
6 inventory (Eyers et al., 2005). The AERO2k inventory was developed by a team at [the](#)  
7 Manchester Metropolitan University (MMU) and indicates [the](#) fuel use and NO<sub>x</sub>, CO<sub>2</sub>, CO,  
8 hydrocarbon and particulate emissions for 2002 and 2025 (projected) with injection height at  
9 a 1°×1 degree spatial resolution on monthly basis. We used their column total CO<sub>2</sub> emissions  
10 to distribute emissions to a single layer. International marine bunker emissions were  
11 distributed at a 0.1°×0.1 degree using an international marine bunker emission map from the  
12 EDGAR v4.1 (JRC, 2017). We decided not to adopt an international and domestic shipping  
13 (1A3d) map from EDGAR v4.2 as it includes domestic shipping emissions that we does not  
14 distinguish.  
15

Deleted:  
Deleted:  
Deleted:  
Deleted:  
Deleted: the

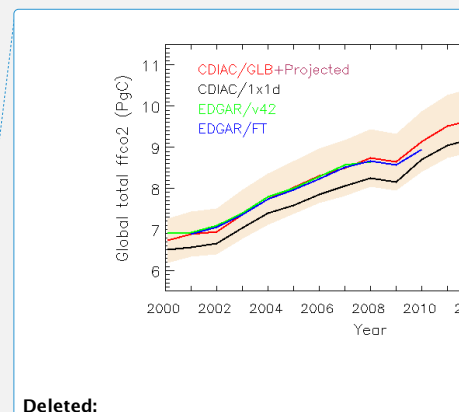
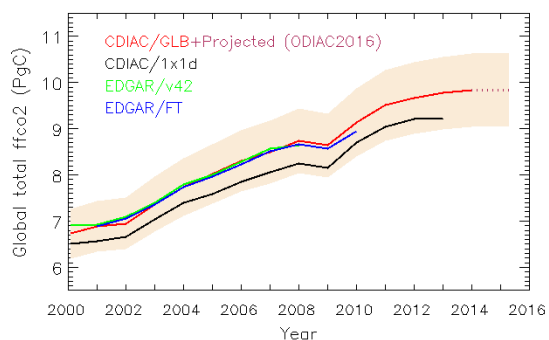
16  
17 **5. Temporal emission disaggregation**  
18

19 The inclusion of the temporal variations is often a key in transport model simulation. For  
20 CO<sub>2</sub> flux inversion, the potential biases in flux inverse emission estimates due to the lack of  
21 temporal profiles was suggested by Gurney et al. (2005). In ODIAC2016, we adopt the  
22 seasonal emission changes developed by Andres et al. (2011). The CDIAC monthly gridded  
23 data include monthly national emissions gridded at a 1°×1 degree resolution (Andres et al.  
24 2011). We normalized the monthly emission fields by the annual total and the applied to our  
25 annual emissions over land. The seasonality in ODIAC2016 is based on the year 2013 version  
26 of the CDIAC monthly gridded emission. The CDIAC monthly emission data do not cover  
27 the recent years. For recent years, we created a climatological seasonality using monthly  
28 CDIAC data from 2000-2010 (excepting 2009 where economic recession happened). Due to  
29 the limited availability of monthly fuel statistical data, Andres et al. (2011) used proxy  
30 country and also seasonality allocated by Monte Carlo simulations. The years between 2000-  
31 2010 were most data rich period and mostly explained by data (see Fig. 1 in Andres et al.,  
32 2011).

Deleted:  
Deleted:

33 Although ODIAC2016 only provides monthly emission fields, users can derive hourly  
34 emissions by applying scaling factors developed by Nassar et al. (2013). The Temporal  
35 Improvements for Modeling Emissions by Scaling (TIMES) is a set of scaling factors which  
36 one can derive weekly emissions and diurnal emissions from any monthly emission data that  
37 you use. Temporal profiles are collected from Vulcan, EDGAR and best available  
38 information and gridded on a 0.25°×0.25 degree (Nassar et al., 2013). TIMES also includes per  
39 capita emissions corrections for Canada (Nassar et al., 2013).  
40  
41

Deleted:  
Deleted:



Deleted:

**Figure 2.** Global emission time series from four gridded emission data: CDIAC (red, 2000-2013) plus projected emissions (dashed maroon, 2014-2015) (values taken from ODIAC2016), CDIAC 1×1 degree (black, 2000-2013), EDGAR v4.2 (green, 2000-2008) and EDGAR v4.2 Fast Track (blue, 2000-2010). The values here are given in the unit of petagram (= giga tonnes) carbon per year. The shaded area indicated in tan is a two-sigma uncertainty range (8%) estimated for CDIAC global total emission estimates by Andres et al. (2014).

1  
2  
3  
4  
5  
6

## 6. Results and discussions

### 6.1 Annual global emissions

7 In Fig. 2, global emission time series from different emission data were compared to give an  
8 idea of agreement among them. We calculated the global total for each year from four gridded  
9 emission data for the period of 2000-2016: CDIAC global total + projection (taken from  
10 ODIAC2016), CDIAC gridded data (hence, no international bunker emissions), two versions  
11 of EDGAR gridded data (v4.2 and FastTrack). The uncertainty range (shaded in tan) is 8% (2  
12 sigma) estimated for CDIAC global by Andres et al. (2014). Those gridded emission data are  
13 often used in global atmospheric CO<sub>2</sub> inversion analysis (e.g. Peylin et al., 2013). To account  
14 for the difference in emission reporting categories (e.g. fuel basis in CDIAC vs. emission  
15 sector basis in EDGAR), the EDGAR totals were calculated as the “total short cycle C”  
16 emissions minus the sum of emissions from agriculture (IPCC code: 4C and 4D), land use  
17 change and forestry (5A, C, D, F and 4E) and waste (6C) (see more details on emission  
18 sectors documented in JRC (2017)). International aviation (1A3a) and navigation (1A3b)  
19 were thus included in values for EDGAR time series. The authors acknowledge the JRC has  
20 updated EDGAR emission time series for 1970-2012 in November 2014 (JRC, 2017). This  
21 study however uses gridded emission data, which are not fully based on the updated emission  
22 estimates, in order to characterize differences from gridded emission data, especially for  
23 potential data users in the modeling community.

24 All four global total values obtained from four gridded emission data agree well within 8%  
25 uncertainty. The difference between ODIAC and CDIAC gridded data (3.3%-5.7%) were

1 largely attributable to the international bunker emissions and global correction. ODIAC  
 2 (where the total was scaled by CDIAC global total) and two versions EDGAR showed minor  
 3 differences in magnitude (0.3%-2.7%) and trend, which are largely attributable to the  
 4 differences in the underlying statistical data (e.g. U.N. Stat vs. EIA from different inventory  
 5 years) and the emission calculation method (fuel basis vs. sector basis). Global total  
 6 estimates at 5-year increments are shown in Table 1. For the year 2014 and 2015, we  
 7 estimated the global total emissions 9.836 and 9.844 PgC. Boden et al. (2017) reported the  
 8 latest estimate for year 2014 global total emission as 9.855 PgC. Our projected 2014 emission  
 9 estimate was lower than the latest estimate by approximately 0.02 PgC (0.2%).

10  
 11  
 12 **Table 1.** Global total emission estimates for year 2000, 2005 and 2010 from four gridded  
 13 emission data (ODIAC2016, CDIAC, EDGAR v4.2 and EDGAR FastTrack). Values for two  
 14 versions of EDGAR emission data were calculated by subtracting emissions from agriculture  
 15 (IPCC code: 4C and 4D), land use change and forestry (5A, C, D, F and 4E) and waste (6C)  
 16 from the total EDGAR CO<sub>2</sub> emissions (total short cycle C).

Year	ODIAC2016	CDIAC national	EDGAR v4.2	EDGAR FT
2000	6727	6506 (-3.3%)	6907 (+2.7%)	N/A
2005	8025	7592 (-5.4%)	8005 (-0.2%)	7959 (-0.8%)
2010	9137	8694 (-4.8%)	N/A	8950 (-2.0%)

18  
 19

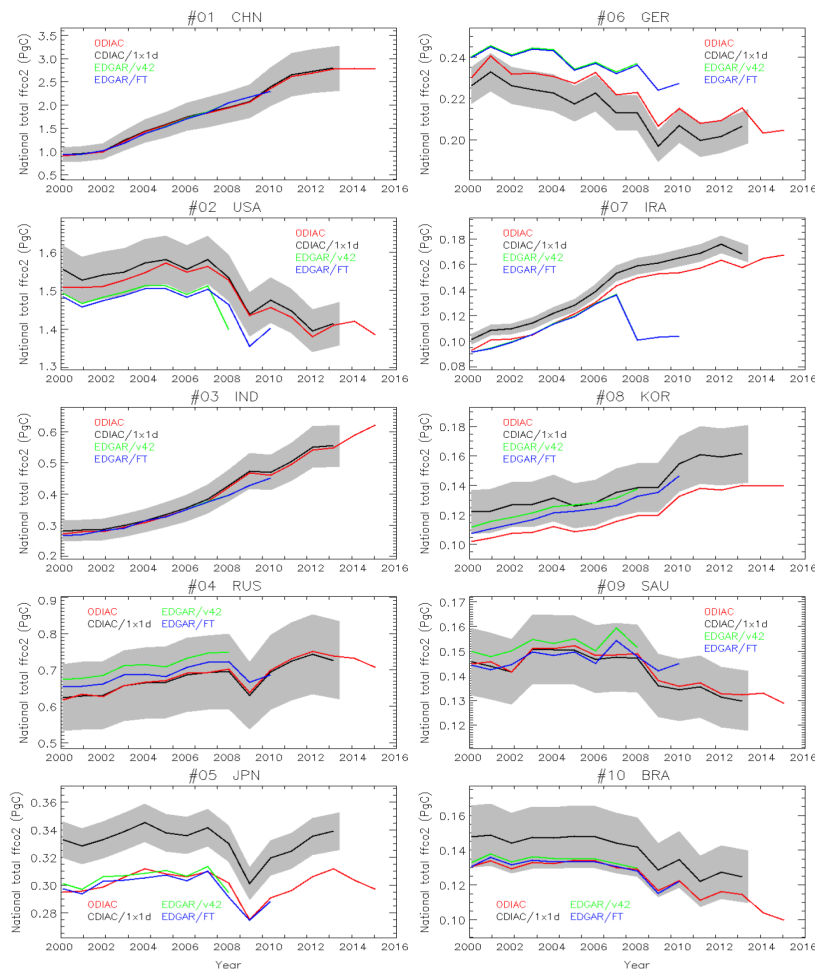


**Figure 3.** National emission time series for top 10 emitting countries (China, U.S., India, Russian Federation, Japan, Germany, Islamic Republic of Iran, Republic of Korea (South Korea), Saudi Arabia and Brazil). The values are given in the unit of peta gram (=giga tonnes) carbon per year. The values are calculated using gridded emission data, not tabular emission data. The national total values in the plots might be thus different from values indicated in the tabular form due to the emission disaggregation. The shaded area in grey indicates a two-sigma uncertainty range estimated by Andres et al. (2014) (see Table 2).

Deleted: 2

1  
2  
3 Fig. 3 shows the same type of comparison as Fig. 2, but for the top 10 emitting countries  
4 (China, US, India, Russian Federation, Japan, Germany, Islamic Republic of Iran, Republic of  
5 Korea (South Korea), Saudi Arabia and Brazil, according to the year 2013 ranking reported  
6 by CDIAC). We aggregated all the four gridded emission fields to a common 1×1 degree field

1 and sampled using the 1×1 degree country mask used in CDIAC emission data development.  
 2 The annual uncertainty estimates for national total emissions (2 sigma) are made following  
 3 the method described by Andres *et al.*, (2014) and values are shown in Table 2. In the  
 4 analysis presented in Fig. 3, emissions from international aviation (1A3a) and navigation  
 5 (1A3b) are excluded. All four national total values sampled from four gridded emission data  
 6 at a 1×1 degree often agree within the uncertainty estimated by Andres *et al.* (2014).  
 7 Systematic differences of ODIAC from CDIAC [gridded data](#) can be largely explained by 1)  
 8 global correction (the total was scaled using CDIAC global total) and 2) the differences in  
 9 emissions disaggregation methods. Although ODIAC is expected to indicate slightly higher  
 10 values than CDIAC [gridded data](#) (often a few percent) because of the global correction (note  
 11 global correction can be negative, despite of the depiction in Fig. 1), ODIAC sometimes  
 12 indicates values lower than CDIAC [gridded data](#) more than few percent (see Japan in Fig. 3 as  
 13 an example). This is due to a sampling error using the 1×1 degree country map in the analysis.  
 14 The aggregated 1×1 degree ODIAC field is slightly larger than that of CDIAC especially  
 15 because of the coastal areas depicted a high-resolution in the original 1×1 km emission field.  
 16 This type of sampling error was discussed in Zhang *et al.* (2014). ODIAC employs a 1×1 km  
 17 coastline and a 5×5 km country mask as described in Oda and Maksyutov (2011). Thus, the  
 18 use of 1×1 degree CDIAC country map results in missing some land mass (hence, CO<sub>2</sub>  
 19 emissions). Similar sampling errors can happen for countries that are physical small and  
 20 island countries, depending on the resolution of analysis. Despite of the sampling errors, the  
 21 authors used the CDIAC 1×1 degree country map to do this comparison analysis with having  
 22 CDIAC [gridded data](#) as a reference. The lower emission indicated by ODIAC or EDGAR in  
 23 this analysis does not always mean the national total emissions are lower. The emission  
 24 estimates at national level often agree well even among different emission inventories (e.g.  
 25 Andres *et al.*, 2012).  
 26  
 27

28 **Table 2.** Annual uncertainty estimates associated with CDIAC national emission estimates.  
 29 The uncertainty estimates were made following the method described by Andres *et al.* (2014).  
 30 The national total emissions for the year 2013 were taken from Boden *et al.* (2016).  
 31

Ranking #	Country	2013 emissions in kTC (% of the global total)	Uncertainty (%)
1	China	2,795,054 (28.6%)	17.5
2	U.S.	1,414,281 (14.5%)	4.0
3	India	554,882 (5.7%)	12.1
4	Russia Federation	487,885 (5.0%)	14.8
5	Japan	339,074 (3.5%)	4.0
6	Germany	206,521 (2.1%)	4.0
7	Islamic Republic of Iran	168,251 (1.7%)	9.4
8	Republic of Korea	161,576 (1.7%)	12.1
9	Saudi Arabia	147,649 (1.5%)	9.4
10	Brazil	137,354 (1.4%)	12.1

32  
 33

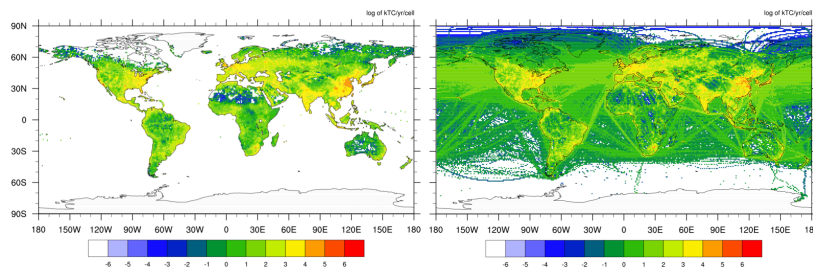


**Figure 4.** Year 2013 global fossil fuel CO<sub>2</sub> emissions distributions from CDIAC (left, 8.36 PgC) and ODIAC (right, 9.78 PgC). The ODIAC emission field was aggregated to a common 1 × 1 degree resolution. The value is given in the unit of log of thousand tonnes C/cell.

1  
2  
3  
4  
5  
6  
7  
8  
9  
10  
11  
12  
13  
14  
15  
16  
17  
18

## 6.2 Global emission spatial distributions

The global total emission fields of CDIAC gridded emission data and ODIAC2016 for the year 2013 (the most recent year CDIAC indicates) are shown in Fig. 4. Emission fields are shown at a common 1×1 degree. The major difference seen between two fields is primarily due to inclusion/exclusion of emissions from international bunker emissions that largely account for the differences indicated in Table 1. A breakdown of ODIAC year 2013 emission field are presented by emission category in Fig. 5. The emission fields for point sources, non-point sources, cement production and gas flaring were produced at a 1×1 km resolution in ODIAC 3.0 model, but as mentioned earlier, we focus on the 1×1 degree version of ODIAC2016 in this manuscript. In CDIAC gridded emission data, the emissions over land are distributed by population data without fuel type distinction. In ODIAC 3.0 model, we have added additional layers of consideration in the emission modeling from the conventional CDIAC model and add the possibility of future improvement with improved emission proxy data.

Deleted: E

Deleted: ose

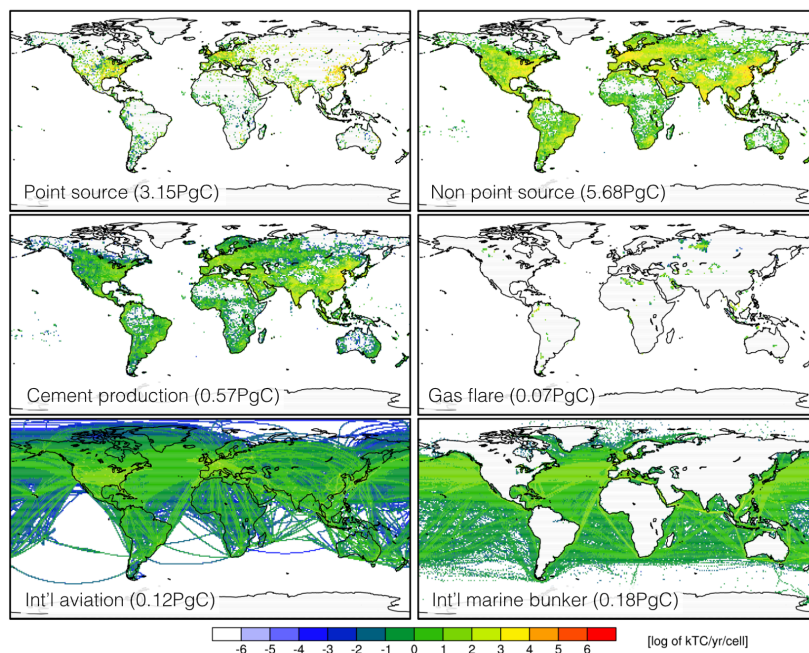


**Figure 5.** Year 2013 global distributions of ODIAC fossil fuel emissions by emission type. The panels show emissions from (from top to the right, then down) point source, non-point source, cement production, gas flaring, international aviation and international shipping. The values in the figures are given in the unit of log of thousand tonnes carbon/year/cell ( $1 \times 1$  degree). The numbers in the brackets are the total for the category emissions in the unit of PgC (total year 2013 emission in ODIAC2016 was 9.78 PgC).

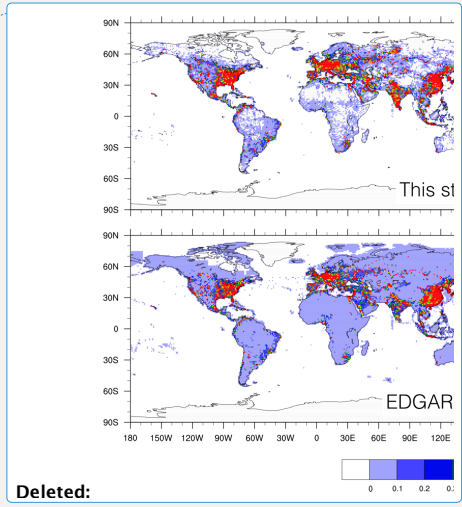
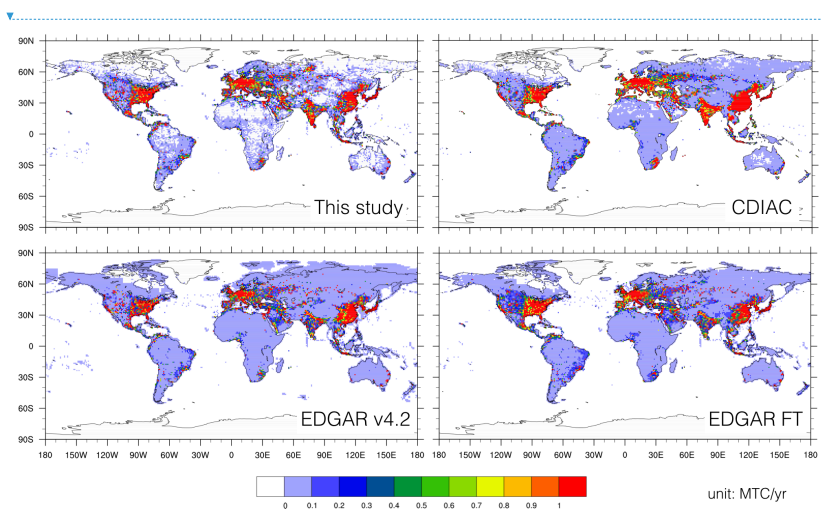
Deleted:  
Deleted:

1  
2  
3  
4  
5  
6  
7  
8  
9  
10  
11  
12  
13  
14  
15  
16  
17  
18

In Fig. 6, we compared the four global gridded products over land and also calculated differences from ODIAC2016 (shown in Fig. 7. [Histograms are presented in Appendix A3](#)). It is often very challenging to evaluate the accuracy and uncertainty of gridded emission data, because of the lack of direct physical measurements at grid scales (Andres et al., 2016). Recent studies have attempted to evaluate the uncertainty of gridded emission data by comparing emission data each other (e.g. Oda et al., 2015; Hutchins et al., 2016). The differences among emission were used as a proxy for uncertainty. However, it is important note that such evaluation does not give us an objective measure of which one is closer to truth, beyond characterizing the differences in emission spatial patterns and magnitudes from methodological viewpoints (e.g. emission estimation and disaggregation). Some of the gridded emission data are partially disaggregated using commercial information, which users are often not authorized to fully disclose the information used and thus makes the comparison even less meaningful and/or significant. Oda et al. (2015) also discussed that emission inter-comparison approaches often do not allow us to evaluate two distinct uncertainty sources (emissions and disaggregation) separately. In addition, because of the use of emission proxy for emission disaggregation (rather than mechanistic modeling), such comparison can be only

1 implemented at an aggregated, coarse spatial resolution. These issues will be further  
 2 discussed in the Section 7.  
 3 Because of the limitation mentioned above, we here compared emission data only to  
 4 characterize the differences that can be explained by the differences in emission  
 5 disaggregation methods. We implemented this comparison exercise using 2008 emission field  
 6 aggregated at a  $1 \times 1$  degree resolution. Year 2008 is the most recent year where all the four  
 7 emission fields are available. The major emission spatial patterns (e.g. emitting regions such  
 8 as North America, Europe and East Asia) are overall very similar as the correlations were  
 9 driven by national emission estimates (which we already saw good agreement earlier), but we  
 10 do see differences due to emission disaggregation at the subnational level. Because of the use  
 11 of nightlight, ODIAC did not indicate emissions over some of the areas (e.g. Africa and  
 12 Eurasia) while others do. Especially, EDGAR has emissions over those areas that are largely  
 13 explained by line source emissions such as transportation. Overall, ODIAC tends to put more  
 14 emissions towards populated areas than suburbs. This is also explained by the lack of line  
 15 sources. In EDGAR v4.2, domestic fishery emissions can be seen, but not in EDGAR FT.  
 16 Even in these two EDGAR versions, we can confirm the subnational differences at United  
 17 States, Europe and China.  
 18  
 19

Deleted: scale



Deleted:

**Figure 6.** Land emissions from ODIAC (upper left), CDIAC (upper right), two versions of EDGAR emission data (v4.2 lower left and v4.2 Fast Track lower right). The units are million tonnes carbon/year/cell ( $1 \times 1$  degree). In addition to excluding emissions from international aviation and marine bunker, some of the sector emissions were subtracted from EDGAR short cycle total emissions to account for the differences in emission calculation methods between CDIAC and EDGAR, as also done earlier. The emission fields for the year 2008 were used.

Deleted:

20

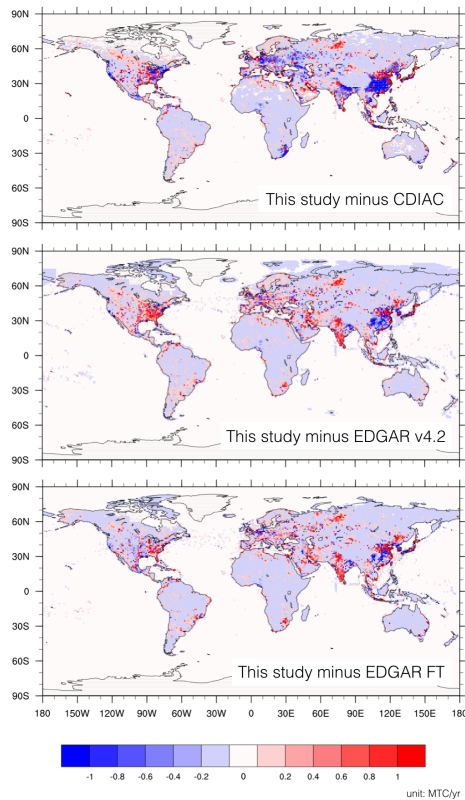


**Figure 7.** ODIAC-other emission data differences. CDIAC (upper right), two versions of EDGAR (v4.2 lower left and v4.2 Fast Track lower right). The units are million tonnes carbon/year/cell ( $1 \times 1$  degree). Note that the differences are defined as ODIAC (this study) minus others. [The histograms of the differences are also presented in Appendix A3.](#)

Deleted: <sp>

Deleted:

Deleted:

Deleted:

1  
2  
3  
4  
5  
6  
7  
8  
9  
10  
11  
12  
13  
14  
15

### 6.3 Regional emission time series.

Fig. 8 shows time series of regional fossil fuel emissions aggregated over 11 land regions defined in the TransCom transport model intercomparison experiment (e.g. Gurney et al., 2002). The global seasonal variation and the associated uncertainty have been presented and discussed in Andres et al. (2011). Here monthly total emission values were calculated for eleven TransCom land regions and presented with the associated uncertainty values (see Table 3). The monthly total values were calculated in both excluding international bunker emissions (hence, land emissions only) and including the emissions. The uncertainty range was calculated by mass weighted uncertainty estimates of countries that fall into the [TransCom](#) regions. The uncertainty ranges shown in Fig. 8 are annual uncertainty plus the monthly profile uncertainty (12.8%, reported by Andres et al., 2011). Monthly time series are presented for land only emissions and land and international bunker emission (here, largely

1 aviation emissions). As described earlier, the emission seasonality was adopted from Andres  
2 et al. (2011). The patterns in [the](#) emission seasonality are often largely characterized by the  
3 large emitting countries within the regions (e.g. U.S. for region 2; China for region 8). Since  
4 Andres et al. (2011) used geographical closeness (also, type of economic systems) to define  
5 proxy countries, the countries in the same TransCom regions can have similar or the same  
6 seasonal patterns in their emissions.

7 As we can see in Fig. 4 (panel plot for aviation emissions), aviation emissions are intense  
8 over North America, Europe and Asia. Global total aviation emission was approximately 0.12  
9 PgC/yr in 2013 and it often does not account for a large portion of the global total (1.2% of  
10 the global total in 2013). However, considering the fact that those emissions are concentrated  
11 in particular areas such as North America, Europe and East Asia, rather than evenly  
12 distributed in space, and often imposed at the surface layer in transport model simulation, care  
13 must be taken to achieve an accurate atmospheric CO<sub>2</sub> transport model simulation (Nassar et  
14 al., 2010). Aviation emissions were often around 0.5-5.1% of the land total emissions over the  
15 most regions, but as large as 12.7% (North American Boreal).

## 17 7. Current limitations, caveats and future prospects

18  
19  
20 As ODIAC emission data product is now used for a wide variety of [the](#) carbon cycle  
21 research (e.g. global, regional inversions, urban emission studies), it would be useful [for the](#)  
22 [users of the ODIAC emission data product](#) to note [and](#) discuss issues, limitations and caveats  
23 in our emission data [that the authors are aware](#). Some of the issues [and](#) limitations are specific  
24 to our study, however the majority of them are often shared by other [existing](#) gridded  
25 emission data and or emission models.  
26

Deleted: s

Formatted: Not Highlight

Deleted: /

Formatted: Not Highlight

Formatted: Not Highlight

Deleted: /

Deleted: as well as modeling frame

Formatted: Not Highlight

Deleted: work

Formatted: Not Highlight

Deleted: /

Deleted: existing

Formatted: Not Highlight

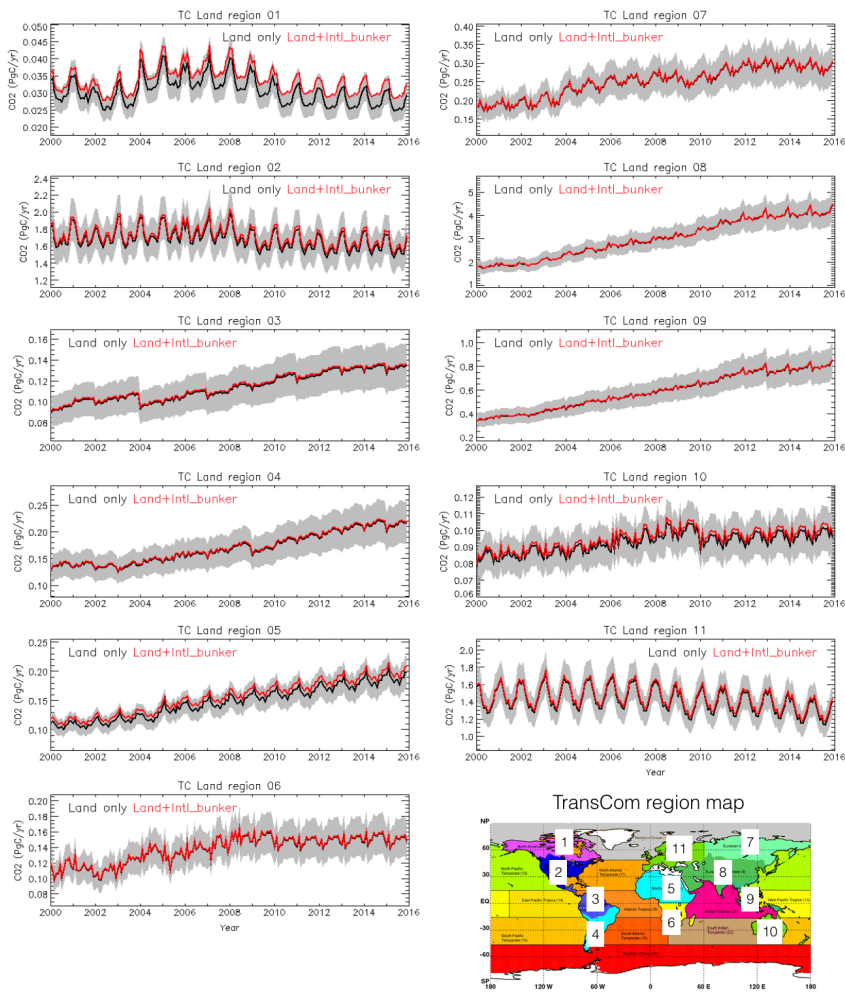


**Figure 8.** Emission time series over inversion analysis land regions defined by the Transport model intercomparison (TransCom) project (Gurney *et al.*, 2002). The TransCom region map (bottom right) is available from [http://transcom.project.asu.edu/transcom03\\_protocol\\_basisMap.php](http://transcom.project.asu.edu/transcom03_protocol_basisMap.php) (last access: 8 November, 2016). Black lines indicate the ODIAC 1×1 degree monthly emissions. The monthly emissions are calculated using the 1×1 degree ODIAC emission data. The uncertainty range was calculated by mass weighted uncertainty estimates of countries that fall into the regions (see Table 3). The uncertainty ranges shown in Fig. 8 are annual uncertainty ranges plus the monthly profile uncertainty (12.8%, reported by Andres *et al.*, 2011). Note scales in the vertical axis are different.

1  
2

**Table 3.** Annual total emission over the TransCom land regions and the associated uncertainty estimates. The total emissions were calculated using the ODIAD2016 gridded emission data. The numbers in the bracket are values including international bunker emissions. The uncertainty estimates were mass weighted values of uncertainty estimates of countries that fall in the regions. Country uncertainty estimates were estimated using the method described Andres et al. (2014). The values were reported as the 2-sigma uncertainty.

Region #	Region name	Uncertainty (%)
1	North American Boreal	3.7
2	North American Temperate	3.7
3	South American Tropical	9.6
4	South American Temperate	12.8
5	Northern Africa	5.1
6	Southern Africa	10.6
7	Eurasian Boreal	12.4
8	Eurasian Temperate	7.8
9	Tropical Asia	11.8
10	Australia	4.0
11	Europe	3.8

## 7.1 Emission estimates

In the production of ODIAC2016, we used several versions/editions of CDIAC estimates (e.g. global estimates, national estimates and monthly gridded data). This could often happen in emission data production, as some of the underlying data are not updated/upgraded at the time of emission data production (we often start updating emission data after new fuel statistical data are released). We sometimes accept the inconsistency and try to use the most up-to-date information available. For example, we could use GCP's emission estimates (e.g. Le Quéré et al., 2016) to constrain the global totals, if CDIAC global total emission estimates are not available. The way we obtained emission estimates for each version is often described in the NetCDF header information of the emission data product. The use of the CARMA power plant estimates for estimating magnitude of point source portion of emissions is hard to eliminate, although ideally this is done using emission estimates that are fully compatible to CDIAC estimates. We are currently examining U.N. statistical data (which CDIAC emission estimates are based on) to assess the ability of explaining power plant emissions.

Deleted: n

## 7.2 Emission spatial distributions

### 7.2.1 Point source emissions

Although the use of the power plant geolocation allowed us to achieve improved high-resolution emission spatial distributions over land (Oda and Maksyutov, 2011), the

1 availability of power plant data is often very limited. For example, CARMA does not provide  
2 power plant emissions and its status (e.g. commission/decommission) every year and  
3 furthermore update/upgrade after their version 3.0 database (which dated 2012). The error in  
4 their power plant geolocation is another issue that has been identified (e.g. Oda and  
5 Maksyutov, 2011; Woodard et al., 2015). In ODIAC, the base year emissions (2007) were  
6 projected and all the power plants were assumed to be active over the period (Oda and  
7 Maksyutov, 2011). There are only few global projects that are collecting power plant  
8 information such as the Global Energy Observatory (GEO,  
9 <http://globalenergyobservatory.org/>) and those can be a useful source of data to improve and  
10 supplement CARMA database. Regionally, CARMA can be evaluated using an inventory  
11 such as the U.S. Emissions and Generation Resource Integrated Database (eGRID) (EPA,  
12 2017). However, it is often difficult to find such a well-constructed and documented  
13 inventory for countries that are actually driving the uncertainty in global emissions (e.g.  
14 China and India).

15 Emissions from cement production (which are currently distributed using nightlight by  
16 Ziskin et al., 2010) and gas flare (which is distributed using gas flare nightlight data by  
17 Elvidge et al., 2009) should be distributed as point sources. For gas flare emissions, we are  
18 examining the use of Nightfire (Elvidge et al., 2013a) to pinpoint active gas flares in timely  
19 manner and improve their emissions spatial disaggregation over the recent years. [Currently,](#)  
20 [the point source emissions in ODIAC do not have an injection height due to the lack of global](#)  
21 [information. This limitation is shared with other existing global emission data products.](#)  
22

### 23 7.2.2 Non-point source emissions

24  
25 Nighttime light data has been an excellent proxy for human settlements (hence, CO<sub>2</sub>  
26 emissions) even at a high spatial resolution, however there are some issues to be discussed.  
27 As mentioned earlier, we used an improved version of calibrated radiance data developed by  
28 Ziskin et al. (2010), but those data are only available to seven data periods over the course of  
29 DMSP years (1992-2013). As we do not believe linearly interpolating the existing nightlight  
30 data over the intervening years is necessarily the best way (as done in Asefi-Najafabady et al.,  
31 2014), the same nightlight data has been used for some periods and thus emission  
32 distributions remain unchanged. We are now examining the use of nightlight data collected  
33 from the Visible Infrared Imaging Radiometer Suite (VIIRS) on Suomi National Polar-  
34 orbiting Partnership satellite (e.g. Elvidge et al., 2013b; Román and Stokes, 2015). VIIRS  
35 instruments do not have several critical issues that the DMSP instrument had (e.g. spatial  
36 resolution, dynamic range, quantization and calibration) (Elvidge et al., 2013b). The fully  
37 calibrated nightlight data can be used to map emission changes in space in timely and  
38 consistent manner.

39 In ODIAC, the disaggregation of non-point emissions is solely done using nighttime light  
40 data for estimating subnational emission spatial distributions and no additional subnational  
41 [emission](#) constrain were applied. Rayner et al. (2010) proposed to better constrain subnational  
42 emission spatial distribution by combining population data, nighttime lights and GDP in their  
43 Fossil Fuel Data Assimilation System (FFDAS) framework. Asefi-Najafabady et al. (2014)  
44 further introduced the use of point source information in their disaggregation, the  
45 optimization in their current framework is however under-constrained by the lack of GDP  
46 information. Without having such optimization, the state level per capita emission estimates  
47 can provide subnational constraints. Nassar et al. (2013) evaluated the per capita emissions in  
48 CDIAC and ODIAC emission data over Canada using the national inventory and found that

1 ODIAC outperformed. However, as the nightlight-population relationship might have a bias  
2 for developing and the least developed countries (Raupach et al., 2010), we would expect we  
3 see significant biases over those countries and the per capita estimates can provide a useful  
4 constraint.

5 As seen in the comparison to other emission data, the major difference from EDGAR  
6 emission spatial distribution was due to the lack of line sources in ODIAC. We do not believe  
7 the result from the emission data comparison can falsify the emission distribution in ODIAC,  
8 as discussed earlier. However, we do expect an inclusion of the line sources would improve  
9 the spatial distributions and emission representations in both cities and rural areas. We are  
10 currently examining the inclusion of transportation network data (e.g. OpenStreetMap) as  
11 proxy for line source emissions to explore the better spatial emission aggregation method.  
12 Oda et al. (2017) recently implemented the idea of adding a spatial proxy for line sources and  
13 improved emission estimates for a U.S. city.

### 14 7.2.3. Aviation emissions

15 We estimated emissions from international aviation from CDIAC using U.N. statistical data.  
16 The emissions are currently provided as a single layer emission field, although it is not  
17 appropriate given the nature of the aviation emissions. Nassar et al. (2010) discussed that the  
18 importance of the three dimensional (e.g. x,y,z) emissions for interpreting CO<sub>2</sub> profile. In  
19 current modeling framework, although we maintain the aviation emission injection height  
20 from AERO2k (reduced to 1km interval), we distribute the emissions to a single layer. As  
21 pointed out by Olsen et al. (2013), AERO2k does not agree with other inventories in height  
22 distribution. With noting the caution, we will examine the use of height information from  
23 AERO2k and other data available to us and do sensitivity analysis using transport model  
24 simulations.  
25  
26  
27  
28

### 29 7.3 Emission temporal profiles.

30 The emission seasonality in ODIAC2016 is based on Andres et al. (2011) and it can be  
31 further extended using the TIMES scaling parameter to hourly scale. We note that the  
32 emission seasonality was based on top 10 emitting countries' fuel statistics and Monte Carlo  
33 simulation (Andres et al., 2011). The emission seasonality for countries other than the top 10  
34 could be less robust. Also, because of the use of Monte Carlo, the seasonality is different over  
35 different editions of monthly emission data. It is also important to note that the repeated use  
36 of climatological (mean) seasonality for the recent years (described in Section 5) could be a  
37 source of uncertainty and biases. Andres et al. (2011) estimated the monthly uncertainty as  
38 12.8% (two sigma) in addition to the annual emission uncertainty. As we often impose fossil  
39 fuel emissions, a care must be taken when applied to inversions. Ultimately, as done by Vogel  
40 et al. (2013), we might be able to evaluate temporal profiles from statistical data and improve  
41 them (but only to limited small locations).  
42  
43

### 44 7.4 Uncertainties associated with gridded emission fields

45 As mentioned earlier, the evaluation of gridded emission data is often very challenging and  
46 most of the emission data study share this difficulty. Although the emission estimates are  
47 made at global and national scales with small uncertainties, (e.g. 8% for global by Andres *et*  
48

Deleted: 2

Deleted: 2

Deleted: an additional

Deleted: over

Deleted: y

1 *al.*, 2014), considerable errors seem to be introduced when [the emissions are](#) disaggregated  
2 (e.g. Hogue et al., 2016; Andres et al., 2016). Andres et al. (2016) for example estimated the  
3 uncertainty associated with CDIAC gridded emission data on a per grid cell basis with an  
4 average of 120% and a range of 4.0 to 190% (2 sigma). Hogue et al. (2016) closely looked at  
5 CDIAC gridded emission data over the U. S. domain and estimated the uncertainty associated  
6 with the 1x1 degree emission grids as  $\pm 150\%$ . Those errors seem to be unique to the  
7 disaggregation method (Andres et al., 2016). Future funding may allow us to pursue a full  
8 uncertainty analysis of the ODIAC emission data/model, akin to the Andres et al. (2016)  
9 approach but accounting for the greater than one carbon distribution mechanisms utilized in  
10 [the](#) ODIAC emission modeling framework. All of the spatially distributed gridded emission  
11 data mentioned in this manuscript suffer from the same basic defect: they use proxies to  
12 spatially distribute emissions rather than actual measurements. In addition, evaluating  
13 emission distributions based on [a](#) nightlight proxy can be challenging as the connection  
14 between CO<sub>2</sub> emissions and proxy is less direct compared to population (e.g. per capita  
15 emissions). A combined use of emission proxy and geolocation data (e.g. power plant  
16 location) would also add additional difficulties to give a comprehensive measure of the  
17 uncertainty because of different type of error/uncertainty sources (e.g. Woodard et al., 2015).  
18 As finer spatial scales are approached, the defect of the proxy approach becomes more  
19 apparent: proxies only estimate emission fields. [The](#) ODIAC data product has been used not  
20 only for global simulations at an aggregated spatial resolution, but also at very high spatial  
21 resolution (e.g. Ganshin et al. 2010; Oda et al. 2012; Lauvaux et al. 2016; Oda et al. 2017).  
22 Thus, [an](#) emission evaluation at a high resolution has become an important task. One  
23 approach we could take for evaluating high-resolution emission fields is comparing to a local  
24 fine-grained emission data product such as Gurney et al. (2012), acknowledging the  
25 limitations of the approach discussed earlier. Another approach would be evaluating emission  
26 data in concentration space, rather than emission space. As reported in Vogel et al. (2013) and  
27 Lauvaux et al. (2016), with radiocarbon measurements and/or good, spatially dense CO<sub>2</sub>  
28 measurements, a high-resolution transport model simulation can provide an objective measure  
29 for emission data evaluations (e.g. model-observation mismatch and emission inverse  
30 estimate).

31 While the quality (i.e. bias and uncertainty) of the gridded emission estimates remains  
32 unquantified for most of the emission data mentioned in this manuscript, the emission data  
33 are still used because sufficient measurements in space and time are not presently available to  
34 offer a better alternative. At very least, we presented [the](#) uncertainty estimates over the  
35 aggregated TransCom land regions. We believe that the regional uncertainty estimates are  
36 highly useful for atmospheric CO<sub>2</sub> inversion modelers, more than uncertainty estimates at a  
37 grid level, which still do not seem to be ready for use. Inversion studies often aggregate flux  
38 estimates over the TransCom land regions to interpret regional carbon budgets, while flux  
39 estimations in their models are done at much higher spatial resolutions (e.g. Feng et al., 2009;  
40 Chevallier et al., 2010; Basu et al., 2013). Taking an advantage of being based on [the](#) CDIAC  
41 estimates, we adopted the updated uncertainty estimates reported by Andres et al. (2016) and  
42 obtained the regional uncertainty estimates. Those estimates are new and readily usable to the  
43 inversion studies especially when interpreting the regional estimates.

#### 44 45 46 **8. Product distribution, data policy and future update**

47 [The](#) ODIAC2016 data product is available from a website hosted by the Center for Global  
48 Environmental Research (CGER), Japanese National Institute for Environmental Studies

Deleted:

Deleted:

(NIES) (<http://db.cger.nies.go.jp/dataset/ODIAC/>, doi: [10.17595/20170411.001](https://doi.org/10.17595/20170411.001)). The data product is distributed under Creative Commons Attribution 4.0 International (CC-BY 4.0, <https://creativecommons.org/licenses/by/4.0/deed.en>). The ODIAC2016 emission data are provided in two file formats: 1) global 1×1 km (30 arc second) monthly file in the GeoTIFF format (only includes emissions over land) and 2) 1×1 degree annual (12 month) file in the NetCDF format (includes international bunker emissions). A single, global 1×1 km monthly GeoTIFF file is about 3.7 GB (compressed to 120 MB). A 1×1 degree single NetCDF annual file is about 6MB.

We update the emission data on annual basis, following a release of an updated global fuel statistical data. Future versions of the emissions data are in principle based on updated version/edition of the underlying statistical data with the same name convention (ODIACYYYY, YYYY= the release year, the end year is YYYY minus 1). In October 2017, we started distributing the updated, year 2017 version of ODIAC data (ODIAC2017, 2000-2016). We primarily focus on years after 2000. Future versions of ODIAC data however might have a longer, extended time coverage.

## 9. Summary

This manuscript describes the year 2016 version of ODIAC emission data (ODIAC2016) and how the emission data product was developed within our upgraded emission modeling framework. Based on the CDIAC emission data, ODIAC2016 can be viewed as an extended version of the CDIAC gridded data with improved emission spatial distributions representations. Utilizing the best available data (emission estimates and proxy), we achieved a comprehensive, global fossil fuel CO<sub>2</sub> gridded emission field that allows data users to impose their CO<sub>2</sub> simulations in a consistent way with many of the global carbon budget analysis. With updated fuel statistics, we should be able to continue producing an updated, future versions of ODIAC emission data product within the same model framework. The capability we developed in this study has become more significant now, given the CDIAC/ORNL's shutdown. Despite of expected difficulties (e.g. discontinued CDIAC estimates), the authors believe that ODIAC could play an important role in delivering emission data to the carbon cycle science community. Limitations and caveats discussed in this manuscript mirror and lead ODIAC's future prospects. The ODIAC emission data product is distributed from <http://db.cger.nies.go.jp/dataset/ODIAC/> with a DOI. Currently the 2017 version of ODIAC emission data (ODIAC2017, 2000-2016) are also available.

## Appendix A

**Table A1.** A list of components in ODIAC2016 and data used in the development.

Component	Data/product name	Description and data source	Reference
Global FFCO <sub>2</sub>	CDIAC global fossil-fuel CO <sub>2</sub> emissions	The year 2016 edition of the CDIAC global total estimates were used to constrain the ODIAC2016 totals. Data available at <a href="http://cdiac.ornl.gov/ftp/ndp030/global.1751_2013.ems">http://cdiac.ornl.gov/ftp/ndp030/global.1751_2013.ems</a> .	Boden et al. (2016)
National	CDIAC	The year 2016 editions of the CDIAC national emission	Boden et al.

Deleted: n  
Deleted: l  
Deleted: The  
Deleted:  
Deleted: n

Deleted: Currently we are working on the year 2017 version of ODIAC data (ODIAC2017) which covers 2000-2016.

Deleted: d

Deleted: the

Deleted: t

Deleted: Currently we are working on  
Deleted: and expecting to release by fall 2017  
Deleted: .

FFCO2	fossil-fuel CO <sub>2</sub> emissions by Nation	estimates are used as a primary input data. Data available at <a href="http://cdiac.ornl.gov/ftp/ndp030/nation.1751_2013.ems">http://cdiac.ornl.gov/ftp/ndp030/nation.1751_2013.ems</a> .	(2016)
Global fuel statistics	BP Statistical review of world energy	The year 2016 edition of <a href="#">the BP statistical data</a> were used to project CDIAc <a href="#">national emissions</a> over the recent years (2014-2015). Data are available at <a href="http://www.bp.com/en/global/corporate/energy-economics/statistical-review-of-world-energy.html">http://www.bp.com/en/global/corporate/energy-economics/statistical-review-of-world-energy.html</a> .	BP (2017)
Monthly temporal variation	CDIAC Gridded Monthly Estimate	The year 2013 version of <a href="#">the CDIAC monthly gridded data</a> were used to <a href="#">the model seasonality</a> in ODIAC2016. Data are available at <a href="http://cdiac.ornl.gov/ftp/fossil_fuel_CO2_emissions_gridded_monthly_v2013/">http://cdiac.ornl.gov/ftp/fossil_fuel_CO2_emissions_gridded_monthly_v2013/</a>	Andres et al. (2011)
<a href="#">Power plant data</a>	<a href="#">CARMA</a>	<a href="#">The CARMA power plant database with geolocation correction described in Oda and Maksyutov (2011). Data available from http://carma.org/.</a>	<a href="#">Wheeler and Ummel et al. 2008</a>
NTL (for non-point emissions)	Global Radiance Calibrated Nighttime Lights	Multiple year NTL data are used to distribute nonpoint emissions. Data are available at <a href="https://ngdc.noaa.gov/eog/dmsp/download_radcal.html">https://ngdc.noaa.gov/eog/dmsp/download_radcal.html</a> .	Ziskin et al. (2010)
NTL (for gas flaring)	Global Gas Flaring <a href="#">Shapefiles</a>	Global gas flaring NTL data are specifically used to distribute gas flaring emissions. Data are available at <a href="http://ngdc.noaa.gov/eog/interest/gas_flares_countries_shapefiles.html">http://ngdc.noaa.gov/eog/interest/gas_flares_countries_shapefiles.html</a>	Elvidge et al. (2009)
Int'l ship tracks	EDGAR v4.1	The international marine bunker emission field in EDGAR v4.1 was used. Data are available at <a href="http://edgar.jrc.ec.europa.eu/archived_datasets.php">http://edgar.jrc.ec.europa.eu/archived_datasets.php</a> .	JRC (2017)
Int'l Aviation flight tracks	AERO2k	Data were used to distributed aviation emissions. More details can be find at <a href="http://www.cate.mmu.ac.uk/projects/aero2k/">http://www.cate.mmu.ac.uk/projects/aero2k/</a> .	Eyers et al. (2005)
Weekly and diurnal cycle	TIMES	This was not a part of ODIAC2016, however it is useful to note that this scaling factors can be used to create weekly and diurnally varying emissions. Data are available at <a href="http://cdiac.ornl.gov/ftp/Nassar_Emissions_Scale_Factors/">http://cdiac.ornl.gov/ftp/Nassar_Emissions_Scale_Factors/</a> .	Nasar et al. (2013)

1  
2  
3  
4

[Appendix A2](#)

[Table A2. A table for the global scaling factor for 2000-2013.](#)

<u>Year</u>	<u>Scaling factor</u>
<a href="#">2000</a>	<a href="#">0.999</a>
<a href="#">2001</a>	<a href="#">1.016</a>
<a href="#">2002</a>	<a href="#">1.008</a>
<a href="#">2003</a>	<a href="#">1.014</a>
<a href="#">2004</a>	<a href="#">1.012</a>
<a href="#">2005</a>	<a href="#">1.022</a>
<a href="#">2006</a>	<a href="#">1.022</a>

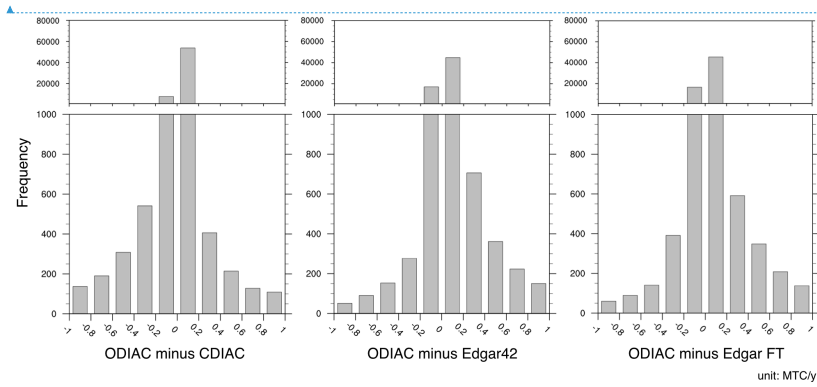
**Formatted:** Font:(Default) Times New Roman, Bold  
Formatted: Font:(Default) Times New Roman

Formatted: Font:Times New Roman

2007	1.016
2008	1.023
2009	1.024
2010	1.015
2011	1.017
2012	1.017
2013	1.025

- Formatted: Font:Times New Roman

Appendix A3



Formatted: Font:11 pt

Fig. A3. A histogram of the inter-emission data differences from ODIAC. Values are given in the unit of million tonnes carbon per year (MTC/yr).

Acknowledgments

TO is supported by NASA Carbon Cycle Science program (Grant # NNX14AM76G). RJA is now retired but this work was sponsored by U.S. Department of Energy, Office of Science, Biological and Environmental Research (BER) programs and performed at the Oak Ridge National Laboratory (ORNL) under U.S. Department of Energy contract DE-AC05-00OR22725. The authors would like to thank Chris Elvidge and Kim Baugh at NOAA/NGDC for providing the nightlight data. The authors also thank Yasuhiro Tsukada and Tomoko Shirai for hosting the ODIAC emission data on the data server at NIES.

References

Andres, R. J., Marland, G., Fung, I., and Matthews, E.: A  $1^\circ \times 1^\circ$  distribution of carbon dioxide emissions from fossil fuel consumption and cement manufacture, 1950–1990, *Global Biogeochem. Cycles*, 10(3), 419–429, doi:10.1029/96GB01523, 1996.

Andres R. J., Gregg J. S., Losey, L., Marland, G., and Boden, T.A.: Monthly, global emissions of carbon dioxide from fossil fuel consumption. *Tellus B*, 63:309-327. doi:10.1111/j.1600-0889.2011.00530.x, 2011.

1  
2 Andres, R. J., Boden, T. A., Bréon, F.-M., Ciais, P., Davis, S., Erickson, D., Gregg, J. S.,  
3 Jacobson, A., Marland, G., Miller, J., Oda, T., Olivier, J. G. J., Raupach, M. R.,  
4 Rayner, P., and Treanton, K.: A synthesis of carbon dioxide emissions from fossil-fuel  
5 combustion, *Biogeosciences*, 9, 1845-1871, doi:10.5194/bg-9-1845-2012, 2012.  
6  
7 Andres, R. J., Boden, T. A., and Higdon, D.: A new evaluation of the uncertainty associated  
8 with CDIAC estimates of fossil fuel carbon dioxide emission. *Tellus B Chem. Phys.*  
9 *Meteorol.* 66, 23616, 2014.  
10  
11 Andres, R. J., Boden, T. A., and Higdon, D. M.: Gridded uncertainty in fossil fuel carbon  
12 dioxide emission maps, a CDIAC example, *Atmos. Chem. Phys. Discuss.*,  
13 doi:10.5194/acp-2016-258, in review, 2016.  
14  
15 Asefi-Najafabady, S., Rayner, P. J., Gurney, K. R., McRobert, A., Song, Y., Coltin, K.,  
16 Huang, J., Elvidge, C., and Baugh, K.: A multiyear, global gridded fossil fuel  
17 CO<sub>2</sub> emission data product: Evaluation and analysis of results, *J. Geophys. Res.*  
18 *Atmos.*, 119, 10,213–10,231, doi:10.1002/2013JD021296, 2014.  
19  
20 Ballantyne, A. P., Alden, C. B., Miller, J. B., Tans, P. P. and White, J. W. C.: Increase in  
21 observed net carbon dioxide uptake by land and oceans during the past 50 years, *Nature*,  
22 488 (7409), 70-72, 2012.  
23  
24 Baker, D. F., Doney, S. C. and Schimel, D. S.: Variational data assimilation for atmospheric  
25 CO<sub>2</sub>. *Tellus B*, 58: 359–365. doi:10.1111/j.1600-0889.2006.00218.x, 2006.  
26  
27 Basu, S., Guerlet, S., Butz, A., Houweling, S., Hasekamp, O., Aben, I., Krummel, P., Steele,  
28 P., Langenfelds, R., Torn, M., Biraud, S., Stephens, B., Andrews, A., and Worthy, D.:  
29 Global CO<sub>2</sub> fluxes estimated from GOSAT retrievals of total column CO<sub>2</sub>, *Atmos. Chem.*  
30 *Phys.*, 13, 8695-8717, doi:10.5194/acp-13-8695-2013, 2013.  
31  
32 Basu, S., Miller, J. B., and Lehman, S.: Separation of biospheric and fossil fuel fluxes of  
33 CO<sub>2</sub> by atmospheric inversion of CO<sub>2</sub> and <sup>14</sup>CO<sub>2</sub> measurements: Observation System  
34 Simulations, *Atmos. Chem. Phys.*, 16, 5665-5683, doi:10.5194/acp-16-5665-2016, 2016.  
35  
36 Boden, T. A., Marland, G., and Andres, R. J.: Global, Regional, and National Fossil-Fuel  
37 CO<sub>2</sub> Emissions. Carbon Dioxide Information Analysis Center, Oak Ridge National  
38 Laboratory, U.S. Department of Energy, Oak Ridge, Tenn., U.S.A. doi  
39 10.3334/CDIAC/00001\_V2015, 2015.  
40  
41 Boden, T.A., G. Marland, and R.J. Andres. 2016. Global, Regional, and National Fossil-Fuel  
42 CO<sub>2</sub> Emissions. Carbon Dioxide Information Analysis Center, Oak Ridge National  
43 Laboratory, U.S. Department of Energy, Oak Ridge, Tenn., U.S.A. doi  
44 10.3334/CDIAC/00001\_V2016  
45  
46 Boden, T.A., G. Marland, and R.J. Andres. 2017. Global, Regional, and National Fossil-Fuel  
47 CO<sub>2</sub> Emissions. Carbon Dioxide Information Analysis Center, Oak Ridge National

1 Laboratory, U.S. Department of Energy, Oak Ridge, Tenn., U.S.A. doi  
2 10.3334/CDIAC/00001\_V2017  
3  
4 Bousquet, P., Ciais, P., Peylin, P., Ramonet, M. and Monfray, P.: Inverse modeling of annual  
5 atmospheric CO<sub>2</sub> sources and sinks 1. Method and control inversion, *J. Geophys. Res.*,  
6 104 (D21), 26161-26178, 1999.  
7  
8 Brioude, J., Angevine, W. M., Ahmadov, R., Kim, S.-W., Evan, S., McKeen, S. A., Hsie, E.-  
9 Y., Frost, G. J., Neuman, J. A., Pollack, I. B., Peischl, J., Ryerson, T. B., Holloway, J.,  
10 Brown, S. S., Nowak, J. B., Roberts, J. M., Wofsy, S. C., Santoni, G. W., Oda, T., and  
11 Trainer, M.: Top-down estimate of surface flux in the Los Angeles Basin using a  
12 mesoscale inverse modeling technique: assessing anthropogenic emissions of CO,  
13 NO<sub>x</sub> and CO<sub>2</sub> and their impacts, *Atmos. Chem. Phys.*, 13, 3661-3677, doi:10.5194/acp-13-  
14 3661-2013, 2013.  
15  
16 BP: Statistical Review of World Energy, available at  
17 [http://www.bp.com/en/global/corporate/energy-economics/statistical-review-of-world-](http://www.bp.com/en/global/corporate/energy-economics/statistical-review-of-world-energy.html)  
18 [energy.html](http://www.bp.com/en/global/corporate/energy-economics/statistical-review-of-world-energy.html) (last access: 6 June 2017), 2017.  
19  
20 Chevallier, F., et al.: CO<sub>2</sub> surface fluxes at grid point scale estimated from a global 21 year  
21 reanalysis of atmospheric measurements, *J. Geophys. Res.*, 115, D21307,  
22 doi:10.1029/2010JD013887, 2010.  
23  
24 Doll, C. N. H., Muller, J.-P., and Elvidge, C. D. Nighttime imagery as a tool for global  
25 mapping of socioeconomic parameters and greenhouse gas emissions, *Ambio*, 29, 157–  
26 162, 2000.  
27  
28 Elvidge, C. D., Baugh, K. E., Dietz, J. B., Bland, T., Sutton, P. C., and Kroehl, H. W.:  
29 Radiance calibration of DMSP-OLS lowLight imaging data of human settlements – a new  
30 device for portraying the Earth’s surface entire, *Remote Sens. Environ.*, 68, 77-88, 1999.  
31  
32 Elvidge, C. D., Imhoff, M. L., Baugh, K. E., Hobson, V. R., Nelson, I., Safran, J., Dietz, J. B.,  
33 and Tuttle, B. T.: Night-time lights of the world: 1994-1995, *J. Photogr. Remote Sens.*, 56,  
34 81–99, 2001.  
35  
36 Elvidge, C. D., Ziskin, D., Baugh, K. E., Tuttle, B. T., Ghosh, T., Pack, D. W., Erwin, E. H.,  
37 Zhizhin, M.: A Fifteen Year Record of Global Natural Gas Flaring Derived from Satellite  
38 Data. *Energies*, 2, 595-622, 2009.  
39  
40 Elvidge, C. D., Zhizhin, M., Hsu, F.-C., and Baugh, K. E.: VIIRS Nightfire: Satellite  
41 pyrometry at night, *Remote Sensing*, 5, 4423-4449, 2013a.  
42  
43 Elvidge, C. D., Baugh, K. E., Zhizhin, M., and Hsu, F.-C.: Why VIIRS data are superior to  
44 DMSP for mapping nighttime lights. *Proceedings of the Asia-Pacific Advanced Network*,  
45 35, 62–69. doi: 10.7125/apan.35.7, 2013b.  
46

1 EPA: Emissions and Generation Resource Integrated Database (eGRID), available at  
2 <https://www.epa.gov/energy/emissions-generation-resource-integrated-database-eGRID>  
3 (last access: 6 June 2017), 2017  
4  
5 Eyers, C. J., Norman, P., Middel, J., Plohr, M., Michot, S., Atkinson, K., and Christou, R. A.:  
6 AERO2k Global Aviation Emissions Inventories for 2002 and 2025, QinetiQ/04/001113,  
7 2005.  
8  
9 Feng, L., Palmer, P. I., Bösch, H., and Dance, S.: Estimating surface CO<sub>2</sub> fluxes from space-  
10 borne CO<sub>2</sub> dry air mole fraction observations using an ensemble Kalman Filter, *Atmos.*  
11 *Chem. Phys.*, 9, 2619-2633, <https://doi.org/10.5194/acp-9-2619-2009>, 2009.  
12  
13 Feng, L., Palmer, P. I., Parker, R. J., Deutscher, N. M., Feist, D. G., Kivi, R., Morino, I., and  
14 Sussmann, R.: Estimates of European uptake of CO<sub>2</sub> inferred from GOSAT  
15 X<sub>CO2</sub> retrievals: sensitivity to measurement bias inside and outside Europe, *Atmos. Chem.*  
16 *Phys.*, 16, 1289-1302, [doi:10.5194/acp-16-1289-2016](https://doi.org/10.5194/acp-16-1289-2016), 2016.  
17  
18 Feng, S., Lauvaux, T., Newman, S., Rao, P., Ahmadov, R., Deng, A., Díaz-Isaac, L. I., Duren,  
19 R. M., Fischer, M. L., Gerbig, C., Gurney, K. R., Huang, J., Jeong, S., Li, Z., Miller, C. E.,  
20 O'Keefe, D., Patarasuk, R., Sander, S. P., Song, Y., Wong, K. W., and Yung, Y. L.: Los  
21 Angeles megacity: a high-resolution land-atmosphere modelling system for urban  
22 CO<sub>2</sub> emissions, *Atmos. Chem. Phys.*, 16, 9019-9045, [doi:10.5194/acp-16-9019-2016](https://doi.org/10.5194/acp-16-9019-2016),  
23 2016.  
24  
25 Feng, L., Palmer, P. I., Bösch, H., Parker, R. J., Webb, A. J., Correia, C. S. C., Deutscher, N.  
26 M., Domingues, L. G., Feist, D. G., Gatti, L. V., Gloor, E., Hase, F., Kivi, R., Liu, Y.,  
27 Miller, J. B., Morino, I., Sussmann, R., Strong, K., Uchino, O., Wang, J., and Zahn, A.:  
28 Consistent regional fluxes of CH<sub>4</sub> and CO<sub>2</sub> inferred from GOSAT proxy  
29 XCH<sub>4</sub>: XCO<sub>2</sub> retrievals, 2010–2014, *Atmos. Chem. Phys.*, 17, 4781-4797,  
30 [doi:10.5194/acp-17-4781-2017](https://doi.org/10.5194/acp-17-4781-2017), 2017.  
31  
32 Ganshin, A., Oda, T., Saito, M., Maksyutov, S., Valsala, V., Andres, R. J., Fisher, R. E.,  
33 Lowry, D., Lukyanov, A., Matsueda, H., Nisbet, E. G., Rigby, M., Sawa, Y., Toumi, R.,  
34 Tsuboi, K., Varlagin, A., and Zhuravlev, R.: A global coupled Eulerian-Lagrangian  
35 model and 1 × 1 km CO<sub>2</sub> surface flux dataset for high-resolution atmospheric  
36 CO<sub>2</sub> transport simulations, *Geosci. Model Dev.*, 5, 231-243, [https://doi.org/10.5194/gmd-](https://doi.org/10.5194/gmd-5-231-2012)  
37 [5-231-2012](https://doi.org/10.5194/gmd-5-231-2012), 2012.  
38  
39 Ghosh, T., Elvidge, C. D., Sutton, P. C., Baugh, K. E., Ziskin, D., and Tuttle, B. T.: Creating a  
40 Global Grid of Distributed Fossil Fuel CO<sub>2</sub> Emissions from Nighttime Satellite  
41 Imagery. *Energies*, 3, 1895-1913, 2010.  
42  
43 Gurney, K. R., Law, R. M., Denning, A. S., Rayner, P. J., Baker, D., Bousquet, P., Bruhwiler,  
44 L., Chen, Y. H., Ciais, P., Fan, S., Fung, I. Y., Gloor, M., Heimann, M., Higuchi, K., John,  
45 J., Maki, T., Maksyutov, S., Masarie, K., Peylin, P., Prather, M., Pak, B. C., Randerson, J.,  
46 Sarmiento, J., Taguchi, S., Takahashi, T., and Yuen, C. W.: Towards robust regional  
47 estimates of CO<sub>2</sub> sources and sinks using atmospheric transport models, *Nature*, 415,  
48 626-630, 2002.

1  
2 Gurney, K. R., Chen, Y.-H., Maki, T., Kawa, S. R., Andrews, A., and Zhu, Z.: Sensitivity of  
3 atmospheric CO<sub>2</sub> inversions to seasonal and interannual variations in fossil fuel  
4 emissions, *J. Geophys. Res.*, 110, D10308, doi:[10.1029/2004JD005373](https://doi.org/10.1029/2004JD005373), 2005.  
5  
6 Gurney, K. R., Mendoza, D., Zhou, Y., Fischer, M., de la Rue du Can, S., Geethakumar, S.,  
7 Miller, C.: The Vulcan Project: High resolution fossil fuel combustion CO<sub>2</sub> emissions  
8 fluxes for the United States, *Environ. Sci. Technol.*, **43**, doi:[10.1021/es900806c](https://doi.org/10.1021/es900806c), 2009.  
9  
10 Gurney K, Razlivanov I, Song Y, Zhou Y. et al. 2012. Quantification of fossil fuel CO<sub>2</sub>  
11 emission on the building/street scale for a large US city. *Environ. Sci. & Technol.* 46:  
12 12194-12202.  
13  
14 Hakkarainen, J., I. Ialongo, and J. Tamminen (2016), Direct space-based observations of  
15 anthropogenic CO<sub>2</sub> emission areas from OCO-2, *Geophys. Res. Lett.*, 43, 11,400–  
16 11,406, doi:[10.1002/2016GL070885](https://doi.org/10.1002/2016GL070885).  
17  
18 Hogue, S., Marland, E., Andres, R. J., Marland, G., and Woodard, D.: Uncertainty in gridded  
19 CO<sub>2</sub> emissions estimates, *Earth's Future*, 4, 225–239, doi:[10.1002/2015EF000343](https://doi.org/10.1002/2015EF000343), 2016.  
20  
21 Hutchins, M.G., Colby, J.D., Marland, G. and Marland, E.: A comparison of five high-  
22 resolution spatially-explicit, fossil-fuel, carbon dioxide emission inventories for the  
23 United States, *Mitig Adapt Strateg Glob Change.*, doi:[10.1007/s11027-016-9709-9](https://doi.org/10.1007/s11027-016-9709-9),  
24 2016  
25  
26 Janardanan, R., Maksyutov, S., Oda, T., Saito, M., Kaiser, J. W., Ganshin, A., Stohl, A.,  
27 Matsunaga, T., Yoshida, Y., and Yokota, T.: Comparing GOSAT observations of  
28 localized CO<sub>2</sub> enhancements by large emitters with inventory-based estimates, *Geophys.*  
29 *Res. Lett.*, 43, 3486–3493, doi:[10.1002/2016GL067843](https://doi.org/10.1002/2016GL067843), 2016.  
30  
31 Janssens-Maenhout G, Dentener F, Van Aardenne J, Monni S, Pagliari V, Orlandini L,  
32 Klimont Z, Kurokawa J, Akimoto H, Ohara, T, Wankmueller R, Battye B, Grano D;  
33 Zuber A, Keating T. EDGAR-HTAP: a Harmonized Gridded Air Pollution Emission  
34 Dataset Based on National Inventories. Ispra (Italy): European Commission Publications  
35 Office; 2012. JRC68434, EUR report No EUR 25 299 - 2012, ISBN 978-92-79-23122-0,  
36 ISSN 1831-9424  
37  
38 JRC: EDGAR – Emissions Database for Global Atmospheric Research, available at  
39 <http://edgar.jrc.ec.europa.eu/> (last access: June 2017), 2017.  
40  
41 Kurokawa, J., Ohara, T., Morikawa, T., Hanayama, S., Janssens-Maenhout, G., Fukui, T.,  
42 Kawashima, K., and Akimoto, H.: Emissions of air pollutants and greenhouse gases over  
43 Asian regions during 2000–2008: Regional Emission inventory in ASia (REAS) version 2,  
44 *Atmos. Chem. Phys.*, 13, 11019-11058, doi:[10.5194/acp-13-11019-2013](https://doi.org/10.5194/acp-13-11019-2013), 2013.  
45  
46 Lauvaux, T., et al.: High-resolution atmospheric inversion of urban CO<sub>2</sub> emissions during the  
47 dormant season of the Indianapolis Flux Experiment (INFLUX), *J. Geophys. Res.*  
48 *Atmos.*, 121, doi:[10.1002/2015JD024473](https://doi.org/10.1002/2015JD024473), 2016.

1  
2 Le Quéré, C., Andrew, R. M., Canadell, J. G., Sitch, S., Korsbakken, J. I., Peters, G. P.,  
3 Manning, A. C., Boden, T. A., Tans, P. P., Houghton, R. A., Keeling, R. F., Alin, S.,  
4 Andrews, O. D., Anthoni, P., Barbero, L., Bopp, L., Chevallier, F., Chini, L. P., Ciais, P.,  
5 Currie, K., Delire, C., Doney, S. C., Friedlingstein, P., Gkritzalis, T., Harris, I., Hauck, J.,  
6 Haverd, V., Hoppema, M., Klein Goldewijk, K., Jain, A. K., Kato, E., Körtzinger, A.,  
7 Landschützer, P., Lefèvre, N., Lenton, A., Lienert, S., Lombardozzi, D., Melton, J. R.,  
8 Metzl, N., Millero, F., Monteiro, P. M. S., Munro, D. R., Nabel, J. E. M. S., Nakaoka, S.-  
9 I., O'Brien, K., Olsen, A., Omar, A. M., Ono, T., Pierrot, D., Poulter, B., Rödenbeck, C.,  
10 Salisbury, J., Schuster, U., Schwinger, J., Séférian, R., Skjelvan, I., Stocker, B. D., Sutton,  
11 A. J., Takahashi, T., Tian, H., Tilbrook, B., van der Laan-Luijkx, I. T., van der Werf, G.  
12 R., Viovy, N., Walker, A. P., Wiltshire, A. J., and Zaehle, S.: Global Carbon Budget 2016,  
13 Earth Syst. Sci. Data, 8, 605-649, doi:10.5194/essd-8-605-2016, 2016.  
14  
15 Maksyutov, S., Takagi, H., Valsala, V. K., Saito, M., Oda, T., Saeki, T., Belikov, D. A., Saito,  
16 R., Ito, A., Yoshida, Y., Morino, I., Uchino, O., Andres, R. J., and Yokota, T.: Regional  
17 CO<sub>2</sub> flux estimates for 2009–2010 based on GOSAT and ground-based CO<sub>2</sub> observations,  
18 *Atmos. Chem. Phys.*, 13, 9351-9373, doi:10.5194/acp-13-9351-2013, 2013.  
19  
20 Marland, G., and Rotty, R. M.: Carbon dioxide emissions from fossil fuels: a procedure for  
21 estimation and results for 1950–1982. *Tellus B*, 36B: 232–261. doi: 10.1111/j.1600-  
22 0889.1984.tb00245.x, 1984.  
23  
24 Myhre, G., Alterskjær, K., and Lowe, D.: A fast method for updating global fossil fuel carbon  
25 dioxide emissions, *Environ. Res. Lett.*, 4, 034012, doi:10.1088/1748-9326/4/3/034012,  
26 2009.  
27  
28 Nassar, R., Jones, D. B. A., Suntharalingam, P., Chen, J. M., Andres, R. J., Wecht, K. J.,  
29 Yantosca, R. M., Kulawik, S. S., Bowman, K. W., Worden, J. R., Machida, T., and  
30 Matsueda, H.: Modeling global atmospheric CO<sub>2</sub> with improved emission inventories and  
31 CO<sub>2</sub> production from the oxidation of other carbon species, *Geosci. Model Dev.*, 3, 689-  
32 716, doi:10.5194/gmd-3-689-2010, 2010.  
33  
34 Nassar, R., Napier-Linton, L., Gurney, K. R., Andres, R. J., Oda, T., Vogel, F. R., and Deng,  
35 F.: Improving the temporal and spatial distribution of CO<sub>2</sub> emissions from global fossil  
36 fuel emission data sets, *J. Geophys. Res. Atmos.*, 118, 917–933,  
37 doi:10.1029/2012JD018196, 2013.  
38  
39 Oda, T., Maksyutov, S., and Elvidge, C. D.: Disaggregation of national fossil  
40 fuel CO<sub>2</sub> emissions using a global power plant database and DMSP nightlight data, *Proc.*  
41 *of the Asia Pacific Advanced Network*, 30, 220-229, 2010.  
42  
43 Oda, T. and Maksyutov, S.: A very high-resolution (1 km×1 km) global fossil fuel  
44 CO<sub>2</sub> emission inventory derived using a point source database and satellite observations  
45 of nighttime lights, *Atmos. Chem. Phys.*, 11, 543-556, doi:10.5194/acp-11-543-2011,  
46 2011.  
47

- 1 Oda, T., Ganshin, A., Saito, M., Andres, R. J., Zhuravlev, R., Sawa, Y., Fisher, R. E.,  
2 Rigby, M., Lowry, D., Tsuboi, K., Matsueda, H., Nisbet, E. G., Toumi, R.,  
3 Lukyanov, A., and Maksyutov, S.: The use of a high-resolution emission dataset in a  
4 Global Eulerian-Lagrangian coupled model, "*Lagrangian Modeling of the Atmosphere*",  
5 AGU Geophysical monograph series, 2012.  
6
- 7 Oda, T. and Maksyutov, S.: Open-source Data Inventory for Anthropogenic CO<sub>2</sub> (ODIAC)  
8 emission dataset, National Institute for Environmental Studies, Tsukuba, Japan.  
9 doi:10.17595/20170411.001, URL: <http://db.cger.nies.go.jp/dataset/ODIAC/>  
10
- 11 Oda, T., Ott, L., Topylko, P., Halushchak, M., Bun, R., Lesiv, M., Danylo, O. and Horabik-  
12 Pyzel, J.: Uncertainty associated with fossil fuel carbon dioxide (CO<sub>2</sub>) gridded emission  
13 datasets. In: *Proceedings, 4th International Workshop on Uncertainty in Atmospheric*  
14 *Emissions*, 7-9 October 2015, Krakow, Poland. Systems Research Institute, Polish  
15 Academy of Sciences, Warsaw, Poland, pp. 124-129. ISBN 83-894-7557-X  
16
- 17 Oda, T, et al: On the impact of granularity of space-based urban CO<sub>2</sub> emissions in urban  
18 atmospheric inversions: A case study for Indianapolis, IN. *Elem Sci Anth*, 5: 28, DOI:  
19 <https://doi.org/10.1525/elementa.146>, 2017  
20
- 21 Olsen, S. C., Wuebbles, D. J., and Owen, B.: Comparison of global 3-D aviation emissions  
22 datasets, *Atmos. Chem. Phys.*, 13, 429-441, doi:10.5194/acp-13-429-2013, 2013.  
23
- 24 Peters, W., Jacobson, A. R., Sweeney, C., Andrews A. E., Conway, T. J., Masrie, K., Miller, J.  
25 B., Bruhwiler, L. M., Petron, G., Hirsch, A. I., Worthy, D. E., van der Werf, G. R.,  
26 Randerson, J. T., Wennberg, P. O., Krol, M. C. and Tans, P. P.: An atmospheric  
27 perspective on North American carbon dioxide exchange: CarbonTracker, *PNAS*,  
28 November 27, 2007, vol. 104, no. 48, 18925-18930, 2007.  
29
- 30 Peylin, P., Law, R. M., Gurney, K. R., Chevallier, F., Jacobson, A. R., Maki, T., Niwa, Y.,  
31 Patra, P. K., Peters, W., Rayner, P. J., Rödenbeck, C., van der Laan-Luijkx, I. T., and  
32 Zhang, X.: Global atmospheric carbon budget: results from an ensemble of atmospheric  
33 CO<sub>2</sub> inversions, *Biogeosciences*, 10, 6699-6720, doi:10.5194/bg-10-6699-2013, 2013.  
34
- 35 Raupach, M. R., Rayner, P. J., and Paget, M.: Regional variations in spatial structure of  
36 nightlights, population density and fossil-fuel CO<sub>2</sub> emissions, *Energy Policy*, 38, 4756–  
37 4764, doi:10.1016/j.enpol.2009.08.021, 2010.  
38
- 39 Rayner, P. J., Raupach, M. R., Paget, M., Peylin, P., and Koffi, E.: A new global gridded  
40 data set of CO<sub>2</sub> emissions from fossil fuel combustion: Methodology and evaluation, *J.*  
41 *Geophys. Res.*, 115, D19306, doi:10.1029/2009JD013439, 2010.  
42
- 43 Román M. O., and Stokes, E. C.: Holidays in Lights: Tracking cultural patterns in demand for  
44 energy services, *Earth's Future*, doi:10.1002/2014EF000285, 2015.  
45
- 46 Saeki, T., Maksyutov, S., Sasakawa, M., Machida, T., Arshinov, M., Tans, P., Conway, T. J.,  
47 Saito, M., Valsala, V., Oda, T., Andres, R. J., and Belikov, D.: Carbon flux estimation for

1 Siberia by inverse modeling constrained by aircraft and tower CO<sub>2</sub> measurements, *J.*  
2 *Geophys. Res. Atmos.*, 118, 1100-1122, doi:10.1002/jgrd.50127, 2013.  
3  
4 Schneising, O., Heymann, J., Buchwitz, M., Reuter, M., Bovensmann, H., and Burrows, J. P.:  
5 Anthropogenic carbon dioxide source areas observed from space: assessment of regional  
6 enhancements and trends, *Atmos. Chem. Phys.*, 13, 2445-2454, doi:10.5194/acp-13-2445-  
7 2013, 2013  
8  
9 Shrai, T., Ishizawa, M., Zhuravlev, R., Ganshin, A., Belikov, D., Saito, M., Oda, T., Valsala,  
10 V., Gomez-Pelaez, A.J., Langenfelds, R. and Maksyutov, S.: A decadal inversion of CO<sub>2</sub>  
11 using the Global Eulerian-Lagrangian Coupled Atmospheric model (GELCA): Sensitivity  
12 to the ground-based observation network, *Tellus B: Chemical and Physical Meteorology*,  
13 69:1, 1291158, DOI: 10.1080/16000889.2017.1291158, 2017  
14  
15 Takagi H., Saeki, T., Oda, T., Saito, M., Valsala, V., Belikov, D., Saito, R., Yoshida, Y.,  
16 Morino, I., Uchino, O., Andres, R. J., Yokota, T., and Maksyutov, S.: On the benefit of  
17 GOSAT observations to the estimation of regional CO<sub>2</sub> fluxes, *SOLA*, 7, 161–164, 2009.  
18  
19 Tans, P.P, Fung, I.Y. and Enting, I.G.: Observational constraints on the global atmospheric  
20 CO<sub>2</sub> budget, *Science*, 247, 1431-1438, 1990.  
21  
22 Thompson, R. L., Patra, P. K., Chevallier, F., Maksyutov, S., Law, R. M., Ziehn, T., Laan-  
23 Luijkx, I. T., Peters, W., Ganshin, A., Zhuravlev, R., Maki, T., Nakamura, T., Shirai, T.,  
24 Ishizawa, M., Saeki, T., Machida, T., Poulter, B., Canadell, J. G., and Ciais, P.: Top-  
25 down assessment of the Asian carbon budget since the mid 1990s, *Nature Comm.*, 7,  
26 2016.  
27  
28 Vogel, F., Tiruchittampalam, B., Theloke, J., Kretschmer, R., Gerbig, C., Hammer, S., and  
29 Levin, I., : Can we evaluate a fine-grained emission model using high-resolution  
30 atmospheric transport modelling and regional fossil fuel CO<sub>2</sub> observations?. *Tellus B*, 65.  
31 doi:<http://dx.doi.org/10.3402/tellusb.v65i0.18681>, 2013.  
32  
33 [Wheeler, D. and Ummel, K.: Calculating CARMA: Global Estimation of CO<sub>2</sub> Emissions](#)  
34 [From the Power Sector, https://www.cgdev.org/publication/calculating-carma-global-](#)  
35 [estimation-co2-emissions-power-sector-working-paper-145, 2008.](#)  
36  
37 Woodard, D., Branham, M., Buckingham, G., Hogue, S., Hutchins, M., Gosky, R., Marland,  
38 G., and Marland, E.: A spatial uncertainty metric for anthropogenic  
39 CO<sub>2</sub> emissions, *Greenhouse Gas Meas. Manage.*, doi:[10.1080/20430779.2014.1000793](https://doi.org/10.1080/20430779.2014.1000793),  
40 2015  
41  
42 Yokota, T., Yoshida, Y., Eguchi, N., Ota, Y., Tanaka, T., Watanabe, H., and Maksyutov, S.:  
43 Global concentrations of CO<sub>2</sub> and CH<sub>4</sub> retrieved from GOSAT: First preliminary results,  
44 *SOLA*, 5, 160–163, doi:10.2151/sola.2009-041, 2009.  
45  
46 Zhang, X., Gurney, K. R., Rayner, P., Liu, Y., and Asefi-Najafabady, S.: Sensitivity of  
47 simulated CO<sub>2</sub> concentration to regridding of global fossil fuel CO<sub>2</sub> emissions, *Geosci.*  
48 *Model Dev.*, 7, 2867-2874, doi:10.5194/gmd-7-2867-2014, 2014

Deleted: .
Deleted: .
Formatted: Font:11 pt
Formatted: Font:11 pt, Subscript
Formatted: Font:11 pt
Formatted: Indent: Left: 0", Hanging: 0.25", Line spacing: multiple 1.15 li
Formatted: Font:11 pt
Formatted: Font:11 pt

1  
2 Ziskin, D., Baugh, K., Hsu, F.-C., Ghosh, T., Elvidege, C.: Methods Used For the 2006  
3 Radiance Lights, *Proc. of the 30<sup>th</sup> Asia-Pacific Advanced Network Meeting*, 131-14, 2010.  
4